TECHNICAL REPORT 2046
August 2014

Hydrodynamic Modeling of Diego Garcia Lagoon

Final Report

P.F. Wang
C. N. Katz
D. B. Chadwick
R. Barua

SSC Pacific
San Diego, CA 92152-5001

TECHNICAL REPORT 2046
August 2014

Hydrodynamic Modeling of Diego Garcia Lagoon

Final Report

P.F. Wang
C. N. Katz
D. B. Chadwick
R. Barua

SSC Pacific
San Diego, CA 92152-5001

SSC Pacific
San Diego, California 92152-5001

K. J. Rothenhaus, CAPT, USN
Commanding Officer

C. A. Keeney
Executive Director

ADMINISTRATIVE INFORMATION

The work described in this report was performed for Naval Facilities Engineering Command Headquarters, by the Energy and Environmental Sciences Group (Code 71750), Space and Naval Warfare Systems Center Pacific (SSC Pacific), San Diego, California.

Released by
C. N. Katz, Head
Energy and Environmental Sciences Group

Under authority of
M. J. Machniak, Head
Advanced Systems & Applied Sciences Division

The citation of trade names and names of manufacturers in this publication is not to construed as official government endorsement or approval of commercial products or services referenced herein.

SB

EXECUTIVE SUMMARY

Upon the request by Naval Facilities Engineering Command (NAVFAC) Headquarters to support a broader investigation into water quality of the Diego Garcia Lagoon, British Indian Ocean Territory, a hydrodynamic modeling effort was conducted by the Energy and Environmental Sciences Group at the Space and Naval Warfare Systems Center Pacific (SSC Pacific). The goal of the study was to simulate and predict water flushing times in the Diego Garcia Lagoon.

The project tasking included both a model study and a field effort. For the modeling study, the Environmental Fluid Dynamics Code (EFDC) model was set up to simulate the hydrodynamics of the lagoon water, including water surface elevation, and flushing times of the lagoon. The field study was conducted to collect hydrodynamic data that was used for an initial validation of model results for the simulation period of 5–18 March 2014.

Dataloggers were deployed at four different locations to measure water surface elevation at 1-min intervals and acoustic Doppler current profilers (ADCPs) were deployed at five stations (ADCP1 through ADCP5) to measure currents during the same time. Measured high-frequency data were processed by a 30-min moving window to filter out high-frequency oscillation before they were compared with model results.

Results of the EFDC model showed that simulated water surface elevations compared well with the measured values at all of the four stations, with mean daily tidal ranges around 112 cm and model–data differences less than 3%. Strongest currents were measured at ADCP1 and ADCP3, with current magnitudes less than 50 cm/s. Model–data differences were between 17% (ADCP3) and -35% (ADCP1), respectively. For the other three stations (ADCP2, ADCP4, and ADCP5), currents were weaker (< 10 cm/s). Model–data differences ranged from -35% (ADCP2), -24% (ADCP5), and -13% (ADCP4), respectively.

Flushing times were predicted for four regions and for the entire lagoon as one water body. Flushing time was defined as the time required to flush 90 or 95% of the initial water mass of the specific region out of the lagoon. Model results showed that Region 1 (the southernmost part) had the longest flushing time of 38 and 43 days for 90 and 95%, respectively, of the initial water mass flushed out of the lagoon. Region 2 had the second-longest flushing time of 33 to 41 days, followed by Region 3 with 22 to 28 days. Region 4 had the shortest flushing time of 19 to 25 days. The flushing time for the entire lagoon ranged from 24 to 32 days for 90 and 95% flushing, respectively.

For a typical discharge scenario in the outer region of the lagoon, vertical mixing in the water column was estimated to complete in about 3 to 4 days. Flushing times were estimated to be 19 to 28.5 days and 17.6 to 27 days for the water-column discharge and the surface discharge scenario, respectively, with 1.5 days shorter for the surface discharge than for the water-column discharge scenario.

It was estimated that only 3.5% of the total discharge mass ends up to the bottom layer for the continuous discharge scenario for a surface discharge. If discharge were to take place only during slack high tide, which conceptually would tend to flush out of the lagoon by the subsequent ebbing tide, only 2.4% of the total discharge mass ends up to the bottom layer, a reduction of 1% of the total discharge mass from the continuous discharge scenario. Strong tidal flushing tends to disperse and discharge the majority of the mass release prior to complete vertical mixing for releases to the surface water in the outer lagoon.

CONTENTS

Figures

Tables

ACRONYMS

ADCP	Acoustic Doppler Current Profiler
CTD	Conductivity, Temperature, and Depth
EFDC	Environmental Fluid Dynamics Code
GPS	Global Positioning System
NAVFAC	Naval Facilities Engineering Command
SMS	Surface Modeling System Software Package
SSC Pacific	Space and Naval Warfare Systems Center Pacific
USEPA	United States Environmental Protection Agency
VP	Vertical Profile
WSE	Water Surface Elevation

1. INTRODUCTION

This report describes results of a hydrodynamic numerical modeling effort to estimate water flushing times in the Diego Garcia Lagoon, British Indian Ocean Territory. Naval Facilities Engineering Command (NAVFAC) Headquarters requested the modeling effort to support a broader investigation into water quality of the lagoon. The work was performed by the Energy and Environmental Sciences Group at the Space and Naval Warfare Systems Center Pacific (SSC Pacific). The project tasking included a field effort to collect hydrodynamic data used to validate the model results. The report describes the project background, field data collection, model setup, and results.

2. BACKGROUND

Diego Garcia is the largest coral reef atoll of more than 60 islands that make up the Chagos Archipelago south of the equator in the central Indian Ocean. It is located at roughly 7˚ south of the equator and at 72˚ east of the Prime Meridian. A coral rim that surrounds a semi-enclosed water body with openings to the ocean at the northern boundary forms the lagoon (Figure 1). The semi-enclosed water body or lagoon is approximately 11 by 9 miles, averages 11.8-m water depth, and can be roughly divided into three major physiographic basins from south to north that are formed and divided by shallow reef ridges. The southernmost basin (Region 1) is the smallest and has the shallowest average water depth of ~ 6.7 m. The next basin to the north (Region 2) is slightly larger and has water depths averaging ~ 8.6 m. The northernmost basin is the largest, and generally has the deepest water depths and averages ~ 13.3 m. The maximum lagoon water depth of 29 m is in this basin. For modeling and flushing time calculations, this northern basin was broken into two north–south regions (Regions 3 and 4).

The deeper northern basin is an area where large military sealift command vessels are anchored on a regular basis. These ships discharge treated effluent and grey water into the lagoon. The estimated total discharge of grey water from these ships into the lagoon is ~ 855,000 gal/mon[1]. Concern about the potential nutrient impacts from these ship discharges prompted a NAVFAC-led investigation of water quality and coral reef health. Hydrodynamic modeling of lagoon waters is one key component of the investigation to understand lagoon circulation, mixing, and flushing rate. Prior to this study, no known datasets on circulation or flushing rate of lagoon waters existed. Therefore, NAVFAC tasked SSC Pacific with implementing a numerical model to simulate the circulation with an explicit goal of using it to calculate lagoon water flushing times. NAVFAC and other researchers will then use the flushing time information to assess water quality conditions and coral reef health.

Researchers use numerical models to simulate the key physical processes of water balance, salt balance, and heat balance, which for coastal lagoons, are influenced most by winds, tides, freshwater inflows, precipitation, and morphology. The key model input parameters therefore include tides, water level, salinity and water temperature, wind velocity, precipitation, and solar radiation, as well as lagoon bathymetry. Most of the necessary data were available for use in the model, though a field effort was conducted to obtain spatial and temporal measurements of current velocity, water level, salinity, and water temperature data that were used for calibration. The following section describes the field data collection and modeling methods.

[1] Personal communication with Maritime Pre-positioning Ship Squadron Two.

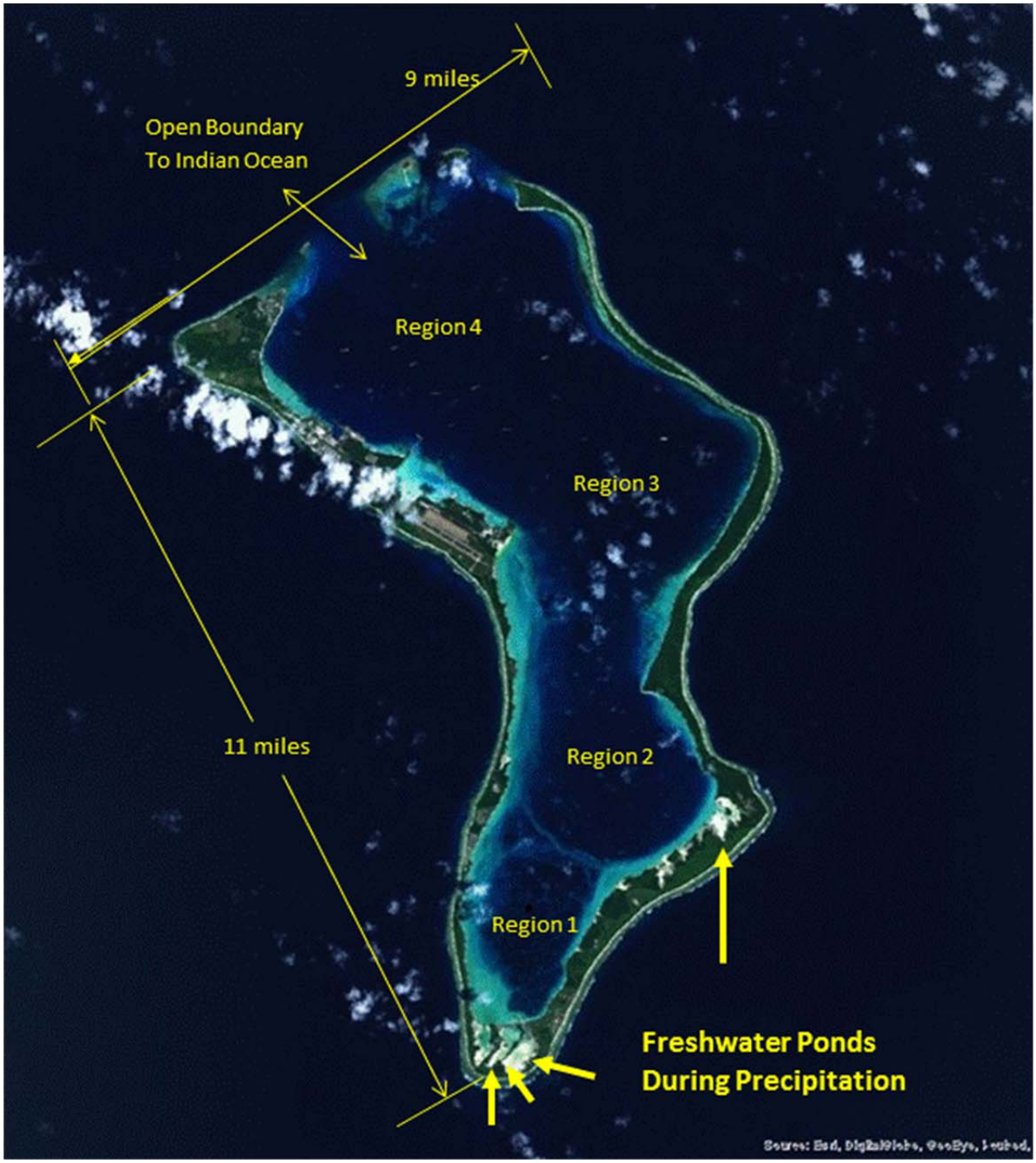

Figure 1. Aerial image of Diego Garcia, BIOT. The opening to the ocean to the north and the three main physiographic basins are also shown. Image © 2014 Google DigitalGlobe, Data SIO, NOAA, U.S. Navy, NGA, GEBCO.

3. METHODS

Methods for the field data collection and hydrodynamic modeling are summarized in the sections below.

3.1 FIELD DATA COLLECTION

Researchers collected hydrodynamic model validation data in the lagoon, 5–19 March 2014, to capture a full 14-day spring-neap tidal cycle period. The dataset included full water column measurements of current velocity using acoustic Doppler current profilers (ADCPs), water level using high-precision pressure sensors, and vertical profiles of seawater salinity and temperature using a standard oceanographic conductivity, temperature, and depth (CTD) profiler. The ADCPs and water level sensors were deployed on 5 March 2014 between ~ 1000 and 1600 hours, and recovered on 19 March 2014 between 0900 and 1200 hours, local time. Vertical profiles of salinity and temperature were measured on 6, 7, 11, 13, and 18 March. Position data for all measurements were recorded with a Global Positioning System (GPS) satellite. Nominal station positions for the three dataset types are shown in Figure 2.

Water velocity measurement locations were designed to capture data from areas representing the connection of the lagoon with the ocean at its mouth, the three main basins of the lagoon, and the narrow transition areas between the ship anchorage to the north and the next basin to the south. Measurements were made along the main axis of the lagoon to intersect the expected main flow regime. Water level was measured at four locations spread out along the shoreline of the lagoon to capture possible changes in the timing of water level elevations with the tide. A pressure sensor (barologger) was also deployed at one location to record atmospheric pressure data to correct the water level data. The CTD vertical profile measurements were designed to monitor water conditions along the main axis under varying tidal stages, including an ebb-flood tide transition, two flood, and one ebb tide condition. Additionally, researchers collected CTD profile data along three cross-axis transects to capture potential changes along the minor axis of each basin. The CTD data were used primarily for model boundary conditions inputs.

3.1.1 Current Velocity

Five Teledyne® RD Instruments ADCPs were placed in the lagoon along an axial transect between the mouth and the southern end of the lagoon. Three of the ADCPs were 1200-kHz units and two were 300- kHz units. All five ADCPs were set to measure current velocity profiles from the top of the unit on the seafloor to the water surface (upward looking) in 1-m bins at a rate of once per minute for the entire 14 days. The ADCPs were marked with a surface buoy used for its recovery (Figure 3). Velocity data were averaged over 50 acoustic measurements made over the 1-min interval. The settings for each unit resulted in a standard deviation of the current speed measurements between 1.9 and 5 cm/s for the 1200- and 300–kHz units, respectively.

Each of the ADCPs was recovered and the data downloaded about halfway through the monitoring period. ADCPs 1, 2, and 3 were moved to slightly shallower water where they were redeployed to better accommodate the instrument depth range. The position changes were less than 260 m from the original positions. The final ADCP positions reported in Table 1 represent an average position measured with a Trimble® GeoXH6000 GPS receiver during deploying and/or redeploying the instruments.

ADCPs were placed along an axial transect of the lagoon at distances of roughly 2.3, 10.7, 13.5, 17.1, and 21.0 km from the mouth (Figure 2). The overall axial distance from the mouth to the back of the lagoon is ~24.0 km. ADCP1 data best represent the outer half of the northernmost basin (Region 4), including flow into and out of the lagoon mouth. ADCP2 best represents the inner half of

the northernmost basin and the area just south of the ship anchorages (Region 3). ADCP3 represents a location with the narrow transitional portion of the lagoon between the main ship anchorage and the middle basin. ADCP4 best represents the middle basin (Region 2) while ADCP5 represents the southernmost basin (Region 1).

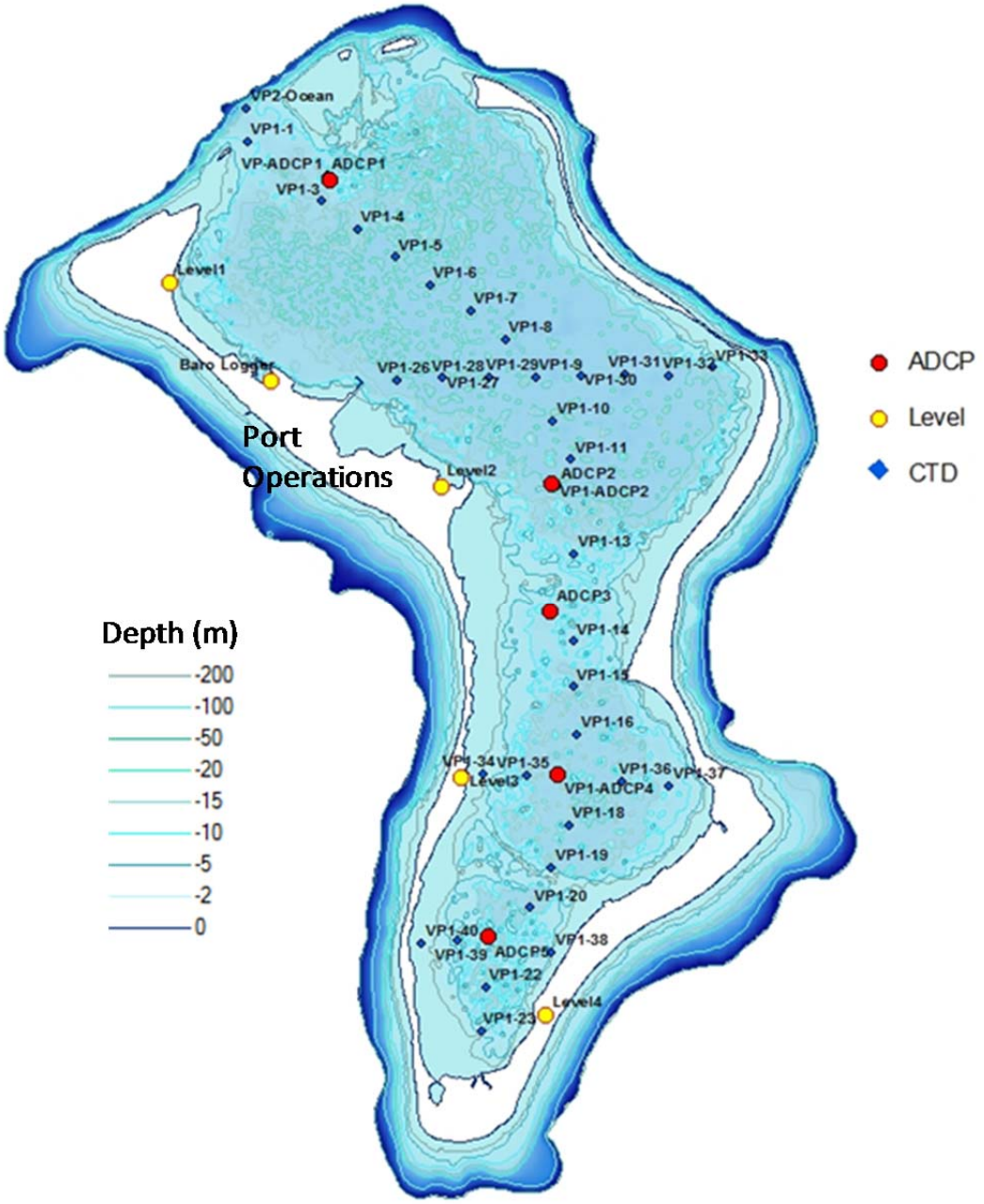

Figure 2. Field data collection station locations.

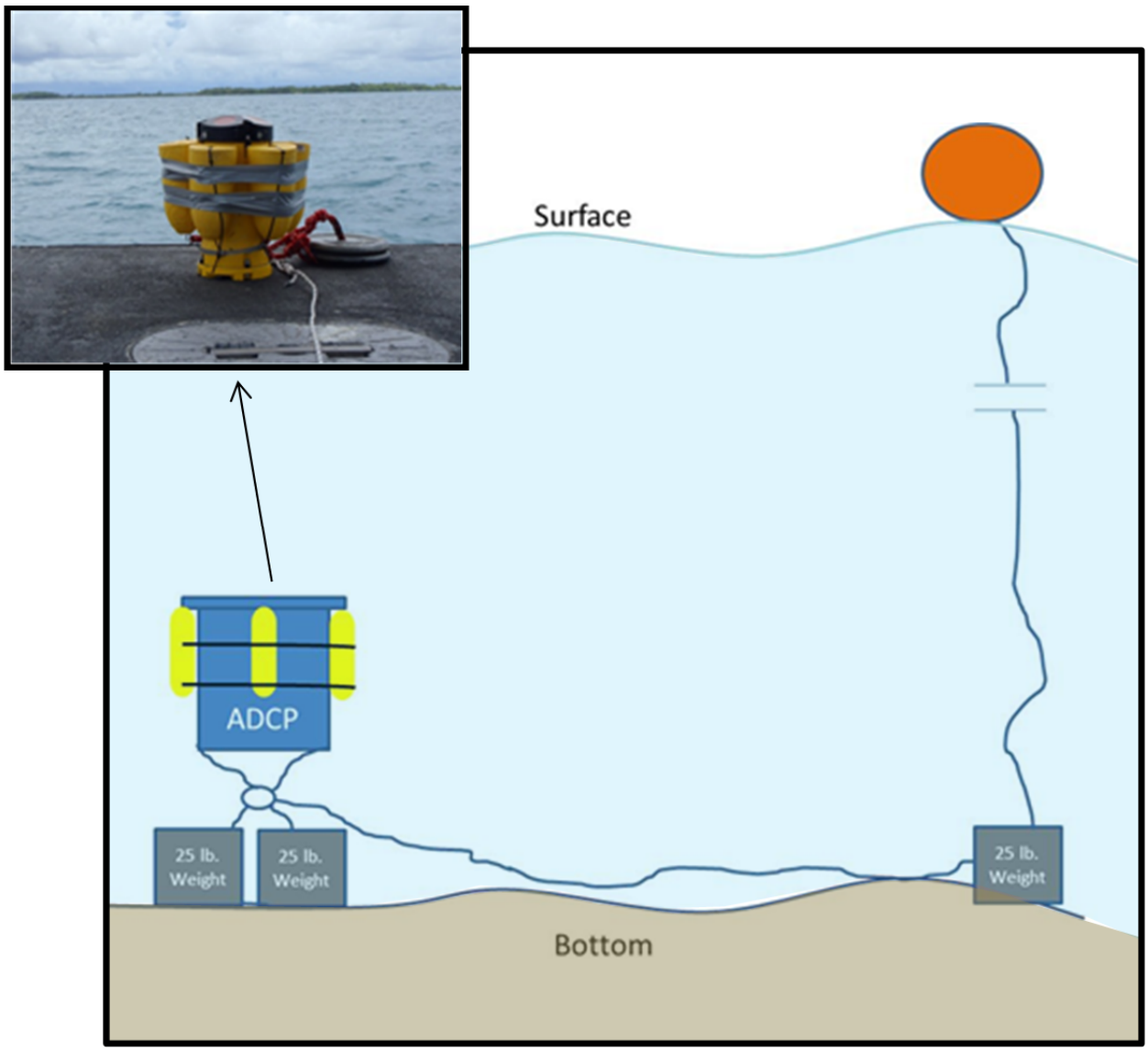

Figure 3. Schematic of ADCP deployment and a unit ready for deployment.

Table 1. ADCP station locations. ADCP1, 2, and 3 were redeployed mid-survey to slightly shallower waters. Positions are based on the average value recorded during the deployment and/or redeployment of the instruments.

Current Velocity Station	Latitude (S)	Longitude (E)
ADCP1	-7.252954	72.403748
ADCP2	-7.314599	72.451404
ADCP3	-7.338626	72.449287
ADCP4	-7.371850	72.450467
ADCP5	-7.404097	72.436691

3.1.2 Water Level

Four Solinst® Edge Model 3001 water level meters (Leveloggers®) were deployed in the waters along the western shore of the lagoon (Figure 2; Table 2). Additionally, a Solinst® Edge Barologger was deployed on land near the small boat basin (Port Operations Shed 457) on the northwest side of the lagoon to measure barometric pressure. The Leveloggers® were placed below the low-tide water surface to measure water level (pressure) during the full survey period of 5–19 March 2014. The Leveloggers® were secured on concrete blocks that were placed on the sediment surface and marked with a small buoy (Figure 4). All Levelogger® positions were manually recorded with the Trimble® GeoXH6000 GPS receiver. All units were recovered once during the monitoring period to download and check data. Leveloggers® 2, 3, and 4 were moved slightly into deeper water early in the monitoring period to ensure the sensors remained below the water surface at low tide.

The Leveloggers® measured total pressure and water temperature once per minute. The measurement of pressure is a combination of barometric pressure and water pressure above the sensor. The actual pressure of just the water level above the sensor was calculated by subtracting the barometric pressure using the data collected by the Barologger. Water level readings from the Leveloggers® were automatically compensated for temperature to obtain the water depth in centimeters.

Table 2. Levelogger® positions. Level 2, 3, and 4 were redeployed shortly after initial deployment to ensure appropriate water depths. Positions are based on the average value recorded during the deployment and/or redeployment of the instruments. The Barologger was placed on land to measure changing barometric pressure.

Level Station	Latitude (S)	Longitude (E)
Level 1	-7.273441	72.374414
Level 2	-7.312710	72.433089
Level 3	-7.371729	72.433559
Level 4	-7.418618	72.444746
Barologger	-7.292434	72.393628

3.1.3 Water Salinity and Temperature

Four sets of vertical depth profiles of salinity and temperature measurements were made using a TROLL® 9500 CTD (S/N 50440) manufactured by In Situ, Inc®. The first set of vertical profile data were collected along 24 axial stations, five of which were co-located with the ADCPs. The additional 18 stations were collected along three cross-lagoon transects, one in each of the three main basins. Figure 2 shows the nominal station locations. Three subsequent sets of vertical profiles were collected from the ocean boundary and at the five ADCP stations along the axis. Surface salinity data were also collected in the Turtle Cove area of the southern lagoon when a gradient of decreasing salinity was observed toward the back of the lagoon.

The CTD was set up to measure and record seawater conductivity, temperature, pressure, depth, and salinity once every 5 sec during the first set of profiles and once every 10 sec for the other three sets. In both cases, the units were lowered manually to collect two data points per meter of water

depth from just below the surface to within 1 m above the bottom (using a weighted line as the indicator; Figure 5). All data were recorded on the unit's internal recorder and its external controller. Station position was nominally measured and manually recorded with the Trimble® GeoXH6000 GPS receiver when the CTD was at the surface, at mid-depth, and at the bottom. The final positions shown in Tables A-1 through A-5 (Appendix A) are based on the average position of the three measurements. The boat clearly drifted up to 110 m during the profiling, though the positions were typically < 25 m of one other. The CTD position data are shown in Appendix A.

Figure 4. Levelogger® attached to concrete block ready for deployment.

3.2 HYDRODYNAMIC MODELING METHODS

The hydrodynamic model, Environmental Fluid Dynamics Code (EFDC), was selected to model the Diego Garcia Lagoon. The model, supported by the United States Environmental Protection Agency (USEPA) for simulation of aquatic systems, is one of the most widely used and technically defensible hydrodynamic models in the world. The most up-to-date three-dimensional (3D) version of the EFDC source code was acquired from EPA Region IV, Atlanta, Georgia, for use in this project. Its governing hydrodynamic equations are 3D, addressing both horizontal and vertical mixing and flow. The model balances water pressure while allowing water density and water surface elevation (WSE) to change with turbulence-averaged equations. This version of the model uses 3D sigma(σ)-coordinates to maintain a constant number of vertical layers throughout the model domain, each with a specified percentage of total depth. The EFDC model allows for drying and wetting in shallow areas by a mass conservation scheme, which is an important capability for the lagoon, which has large areas mostly to the south that become dry during low tide.

As described previously, numerical models simulate the key physical processes of water balance, salt balance, and heat balance, which for coastal lagoons are influenced most by winds, tides, and morphology. The key model input parameters therefore include tides, water level, salinity and water temperature, wind velocity, precipitation, solar radiation, and lagoon bathymetry. Most of the necessary data were available though the field effort conducted to obtain spatial and temporal

measurements of current velocity, water level, salinity, and water temperature data that were used for model validation.

Figure 5. CTD unit ready for deployment.

3.2.1 Bathymetry and Model Grid

Bathymetry data were acquired from TCarta Marine LLC. The dataset is composed of sounding data collected between 1967 and 1997. The dataset included 2782 sounding data points that were interpolated onto a 50-m spatial resolution grid within the lagoon and 200-m grid resolution immediately outside the lagoon (Figure 6). These data were used to generate the model grid depth values.

Researchers used the grid generator software, *gefdc.f*, to generate orthogonal curvilinear grid for EFDC. The model grid includes the entire lagoon domain and part of the ocean boundary outside the mouth. The depth of each grid cell was determined by averaging the bathymetric data provided by TCarta Marine LLC within each model grid cell.

A geo-referenced image of Diego Garcia, imported from ArcMap 10, was used as a background to plot the grid cells. The grid was generated interactively through the surface modeling system (SMS)

interface, making a best effort to maintain orthogonality as well as accuracy. The boundary was fitted as accurately as possible, using the background image as a reference. The cell configuration and boundary coordinates generated in SMS were input to EFDC along with the depth data to calculate an inverse distance-weighted mean depth at each of the cell centers. The final model grid is a 25-column by 75-row, curvilinear orthogonal grid containing 1152 water cells with an approximate cell size of 400 m x 400 m.

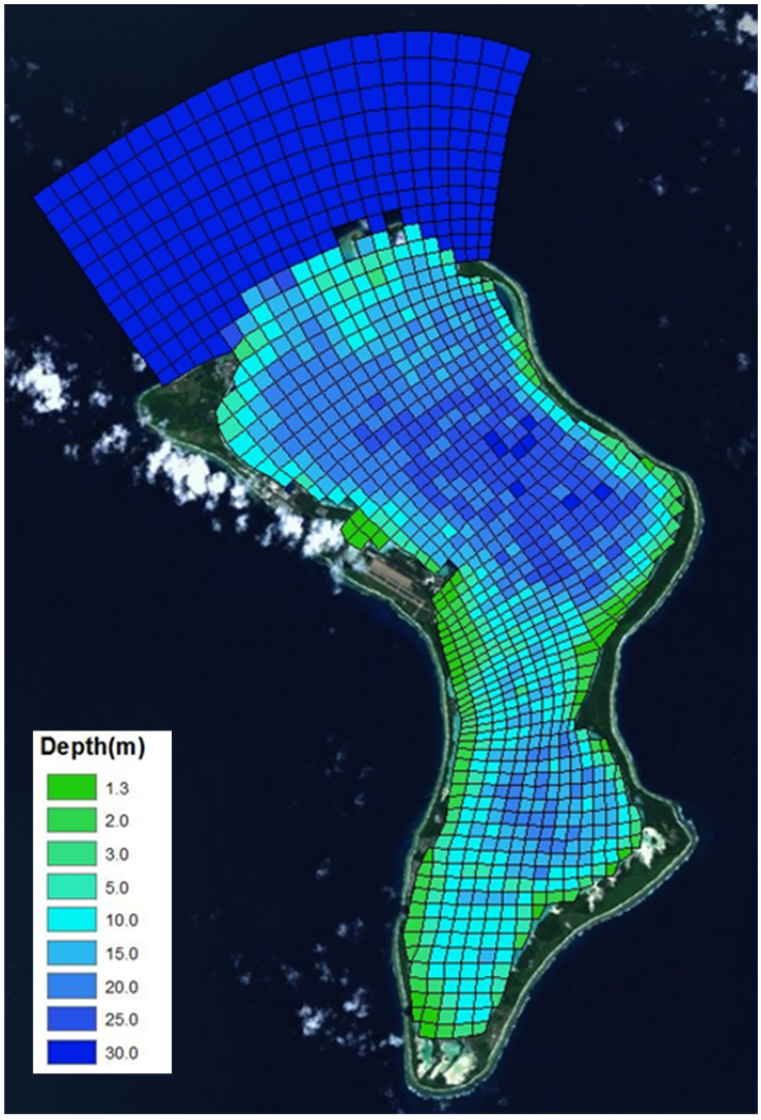

Figure 6. The EFDC model grid for Diego Garcia Lagoon with grid-cell averaged bathymetry. Image © 2014 Google DigitalGlobe, Data SIO, NOAA, U.S. Navy, NGA, GEBCO.

3.2.2 Ocean Boundary Condition

Hydrodynamic exchange and tidal forcings of the lagoon are driven primarily by ocean tides that enter into the lagoon from the mouth at the northern boundary. Tide data were acquired from a tide gage operated by Jason Klem of the University of Hawaii Sea Level Center. The data were collected as part of the Intergovernmental Oceanographic Commission and provided under the Sea Level Station Monitoring Facility (http://www.ioc-sealevelmonitoring.org/index.php). The tide gage is

located on the main pier at the Port Operations Facility to the north along the eastern shore (-7.2333 S, 72.4333 E; Figure 1). Dr. Klem provided 15-min validated tide data for 2013 and January through March 2014, covering the time period of the field measurements. The data were in units of meters relative to mean sea level.

3.2.3 Freshwater Boundary Condition

Researchers assumed that the main source of freshwater to the Diego Garcia Lagoon was precipitation and runoff from the small land mass of the atoll. The EFDC model requires precipitation data, which are supplied to the entire model domain during precipitation and flow of freshwater and associated salinity and temperature from this "freshwater boundary" of watershed runoff. All freshwater input was therefore calculated based on the precipitation data and the land surface areas of the four large ponding areas located along the shoreline of the southernmost lagoon region (Figure 1). For this study, the precipitation data (in/hr) were multiplied by the surface areas of the ponds, which were used as the freshwater inflows to the lagoon during the simulation period. This provided a first-order estimation of the local freshwater loads, which may be underestimated. The freshwater salinity was assumed to be 0.5 psu. The freshwater temperature was assumed to be equal to the air temperature obtained in the meteorological dataset described in Section 3.2.4.

3.2.4 Meteorology

Meteorological data for 2013 through March 2014 were obtained from the Navy's Meteorology and Oceanography Office located adjacent to the airport (near Port Operations) on Diego Garcia. Wind speed and direction, precipitation, air temperature, barometric pressure, and cloud cover data were collected hourly. The dataset also included daily minimum, maximum, and average climate conditions from 2004 through March 2014. No solar radiation data were available for Diego Garcia.

Preparation of weather input files (aser.inp and wser.inp) for 2013 and March 2014 were created from archived data sets hosted by the National Oceanic and Atmospheric Administration (NOAA), Weather Underground, Inc., and the Department of Energy's Atmospheric Radiation Measurement (ARM) Program. Specifically, quality controlled datasets for 2013 and March 2014 from the Diego Garcia airport weather station were obtained from the NOAA Quality Controlled Local Climatological Data (QCLCD) archive. Precipitation data for March 2014 was collected from Weather Undergrounds's online dataset for the Diego Garcia airport. Solar radiation datasets were obtained from the ARM database for the Manus Island station at roughly the same latitude as Diego Garcia and for the appropriate time period. The locations of the stations reporting the accessed data are shown in Figure 7

Each input file was created to represent hourly conditions in the region. Specific data required by the EFDC model were barometric pressure (mbar), dry bulb temperature (° C), relative humidity, rainfall rate (m/s), evapotranspiration rate (m/s), net solar shortwave radiation ($J/m^2/s$), cloud cover, wind speed (m/s), and wind direction. Data from the Diego Garcia airport provided barometric pressure, dry bulb temperature, dewpoint, precipitation, cloud cover, wind speed, and wind direction. Relative humidity was calculated based on established correlations between relative humidity and dewpoint (Lawrence, 2005). Evapotranspiration estimates were made using a version of the Modified Penman Equation (CIMIS, 2014). Solar radiation measurements were obtained from the ARM dataset originating from Manus Island.

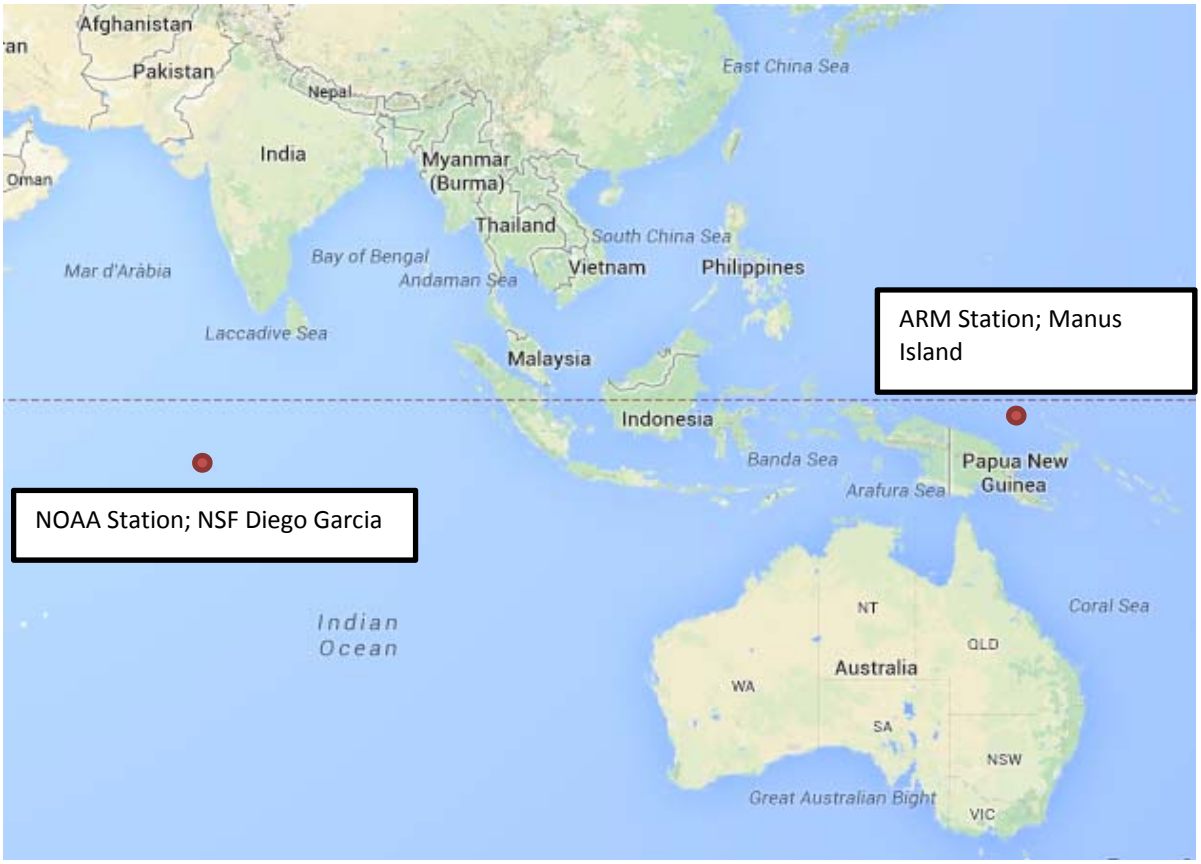

Figure 7. Locations of where data were collected for creating EFDC input files. Image © 2014 Google.

4. MODEL RESULTS

Model simulations were conducted 1–30 March 2014. The model simulations were compared with observed water surface elevation and current data collected 5–19 March 2014 at the four Levelogger® and five ADCP stations described earlier.

4.1 WATER SURFACE ELEVATION

Water surface elevation of the lagoon dictates the volume of water in the lagoon at any specific time. It is a hydrodynamic property governed by the interaction between the ocean water, geometry, bathymetry, and freshwater inflow. Comparison of modeled versus measured water surface elevation provides a primary basis for assuring that the volume of water moving through the lagoon is accurately predicted by the model and provides an indication that the model is correctly simulating the hydrodynamics of the lagoon.

Field data of water surface elevations were recorded once per minute. To compare with the model results, the field data were averaged with a 30-minmoving-average filter. An example of 1-min raw data versus the 30-min average data is shown in Figure 8. The source of the high-frequency noise is unknown but is suspected to be related to high instrument sensitivity and/or wave motions unaccounted for in this study.

Since measured water surface elevations are based on different datum, daily tidal ranges (daily maximum and daily minimum of water surface elevation) were averaged over the simulation period and the mean daily tidal range was used for model–data comparison.

The mean daily tidal range was calculated for all four Leveloggers® and with the model. Results of the comparison are in Table 3 and Figure 9 through Figure 12. The difference between model and measured level increased slightly between the mouth and the back of the lagoon from a slight under-prediction at LL1 (1.4%) in the north to a slight overprediction at LL4 (2.9%) in the south. The overall difference between model and measured levels averaged 2.3%. The good agreement in model and observed data are shown in the graphical plots. The graphical plots have different y-axes because the field data were measured relative to the bottom while modeled data were calculated relative to mean sea level.

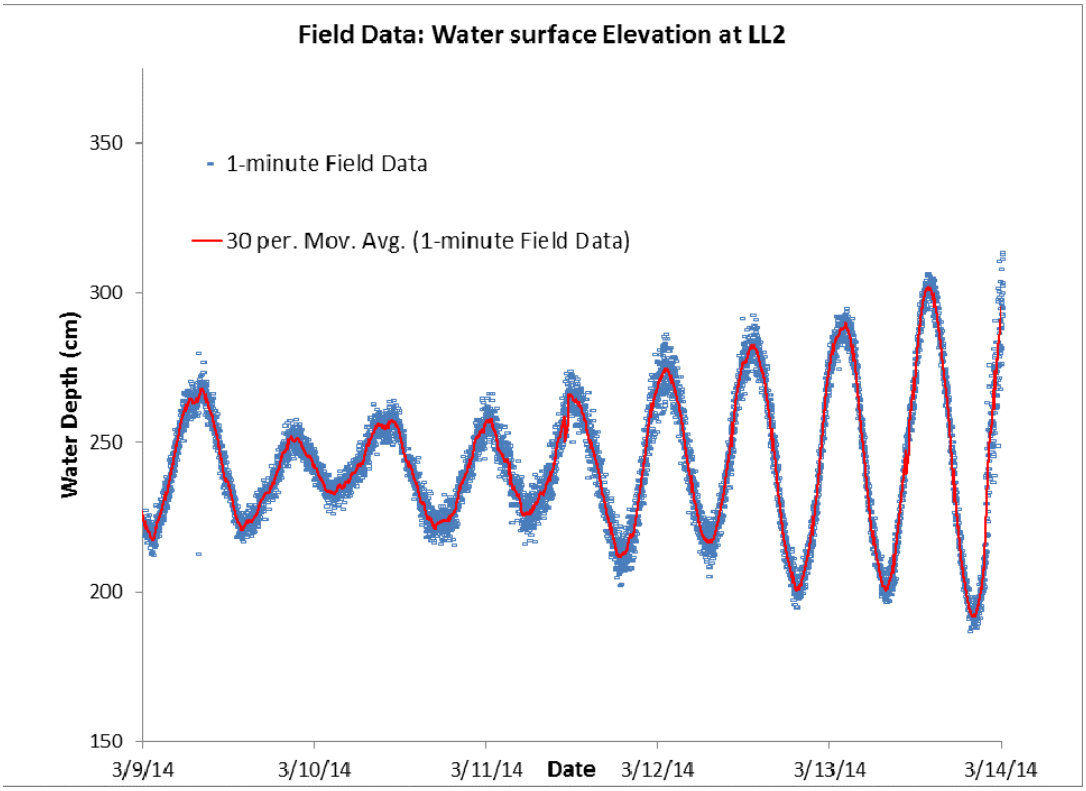

Figure 8. Measured water surface elevation at LL2 (9–14 March 2014). Raw data in blue symbols, 30-min moving averages in red line.

Table 3. Mean daily tidal range between model and field data.

Level Locations	Mean Daily Tidal Range (cm)	
	Model	Field Data
LL1	111	112.6
LL2	115	112.3
LL3	119	116.0
LL4	120	116.6

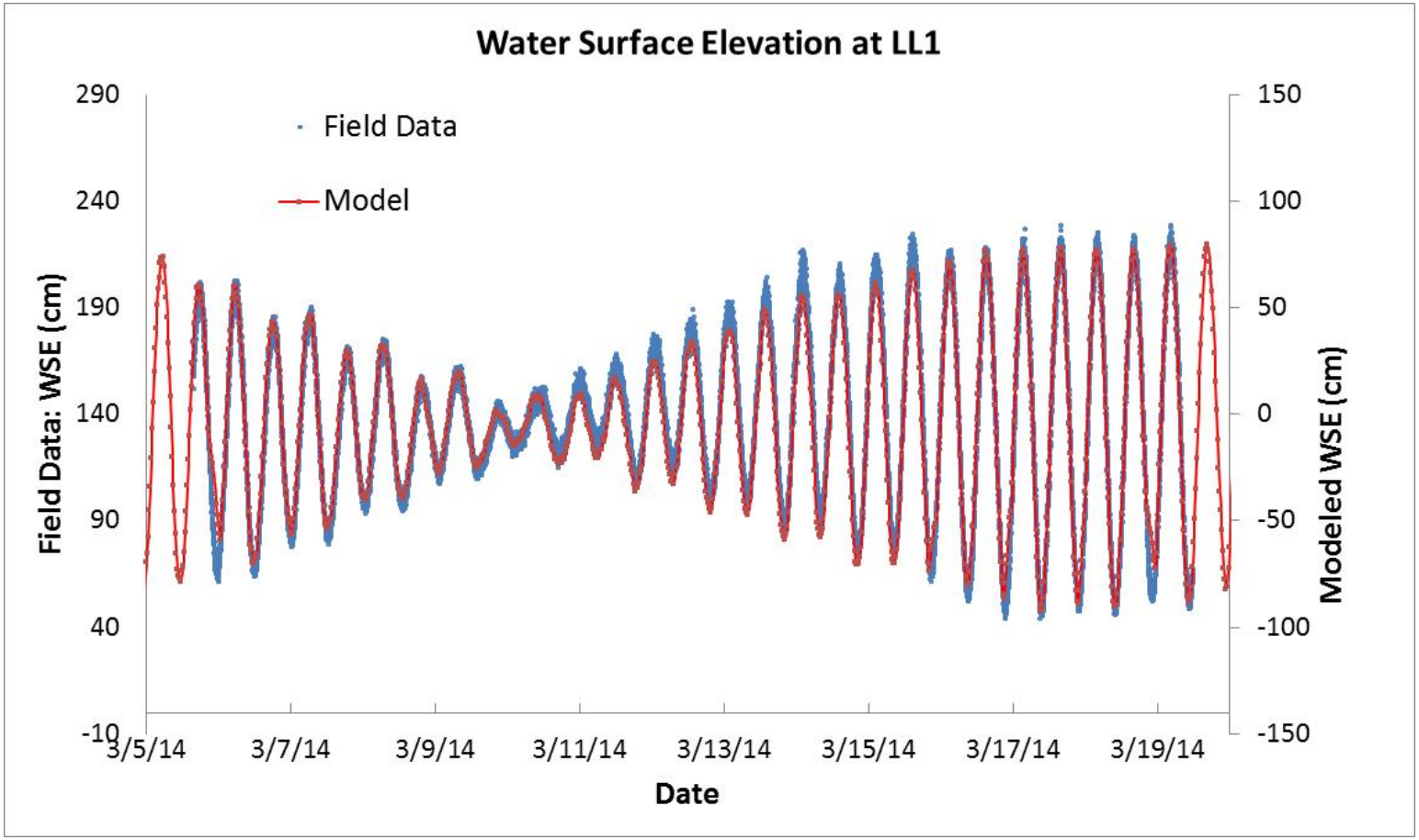

Figure 9. Simulated and measured water surface elevation at LL1 (30-min averaged). Field data were measured relative to the bottom while modeled data were measured relative to mean sea level.

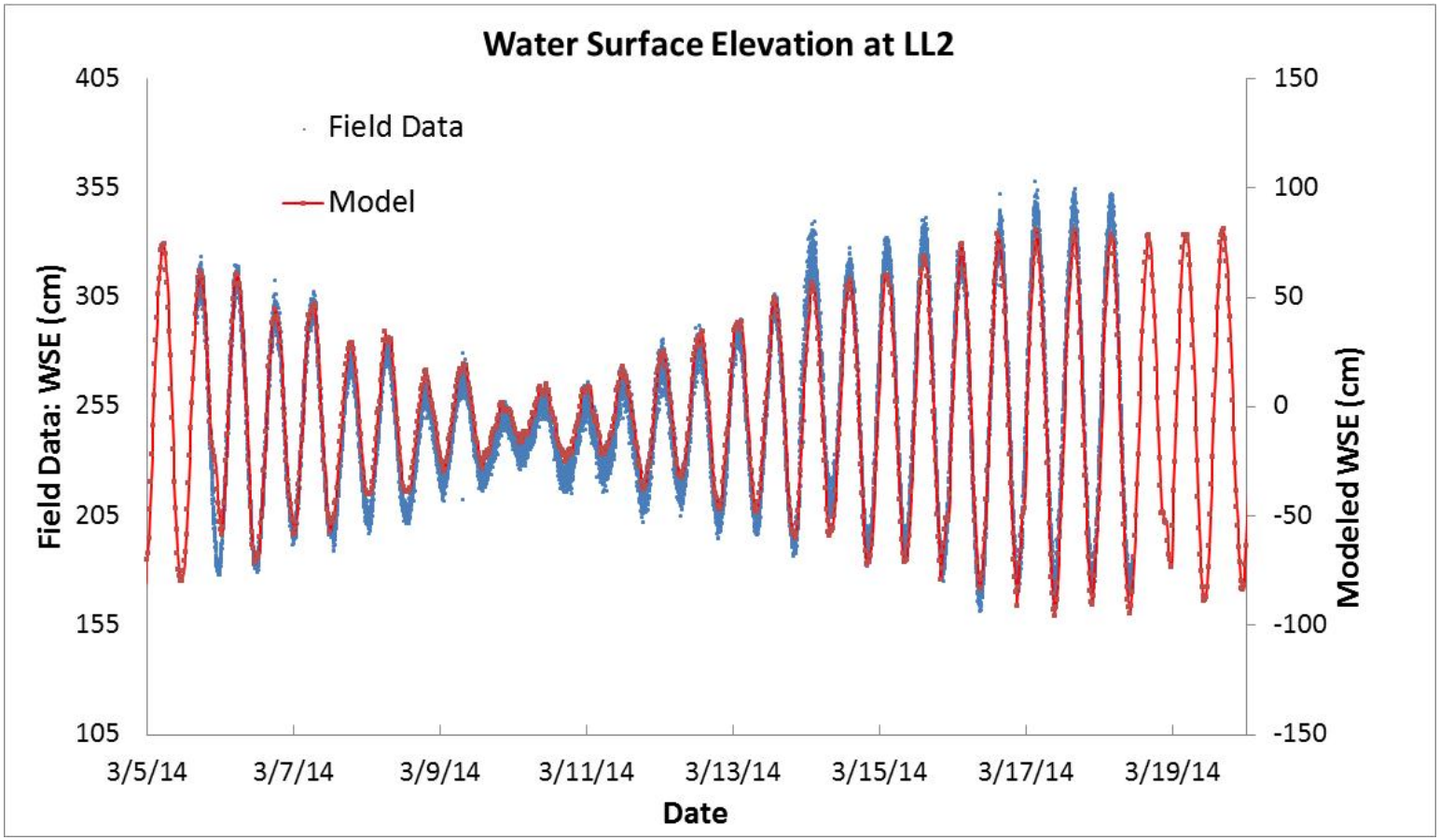

Figure 10. Simulated and measured water surface elevation at LL2 (30-min averaged). Field data were measured relative to the bottom while modeled data were measured relative to mean sea level.

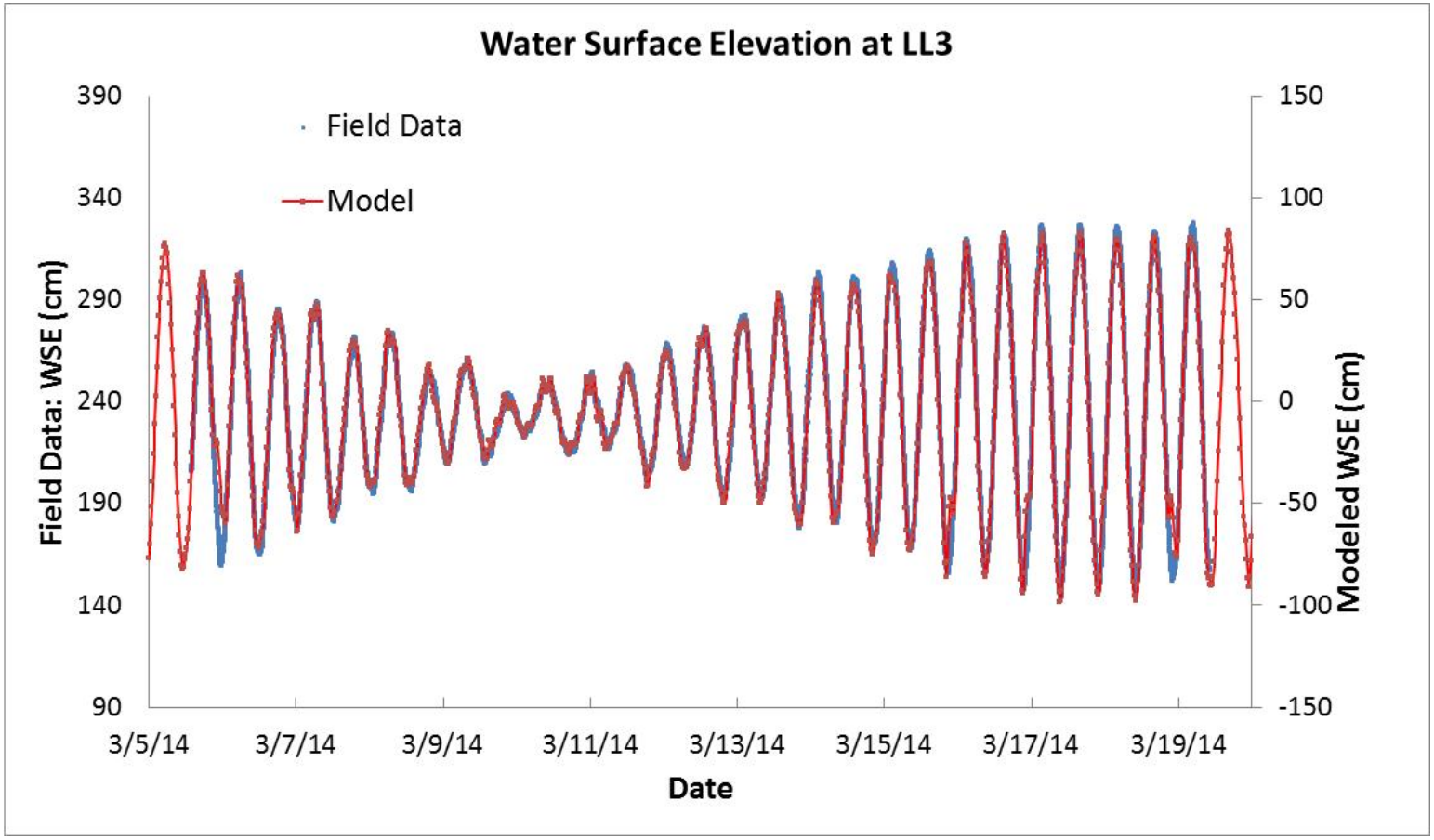

Figure 11. Simulated and measured water surface elevation at LL3 (30-min averaged). Field data were measured relative to the bottom while modeled data were measured relative to mean sea level.

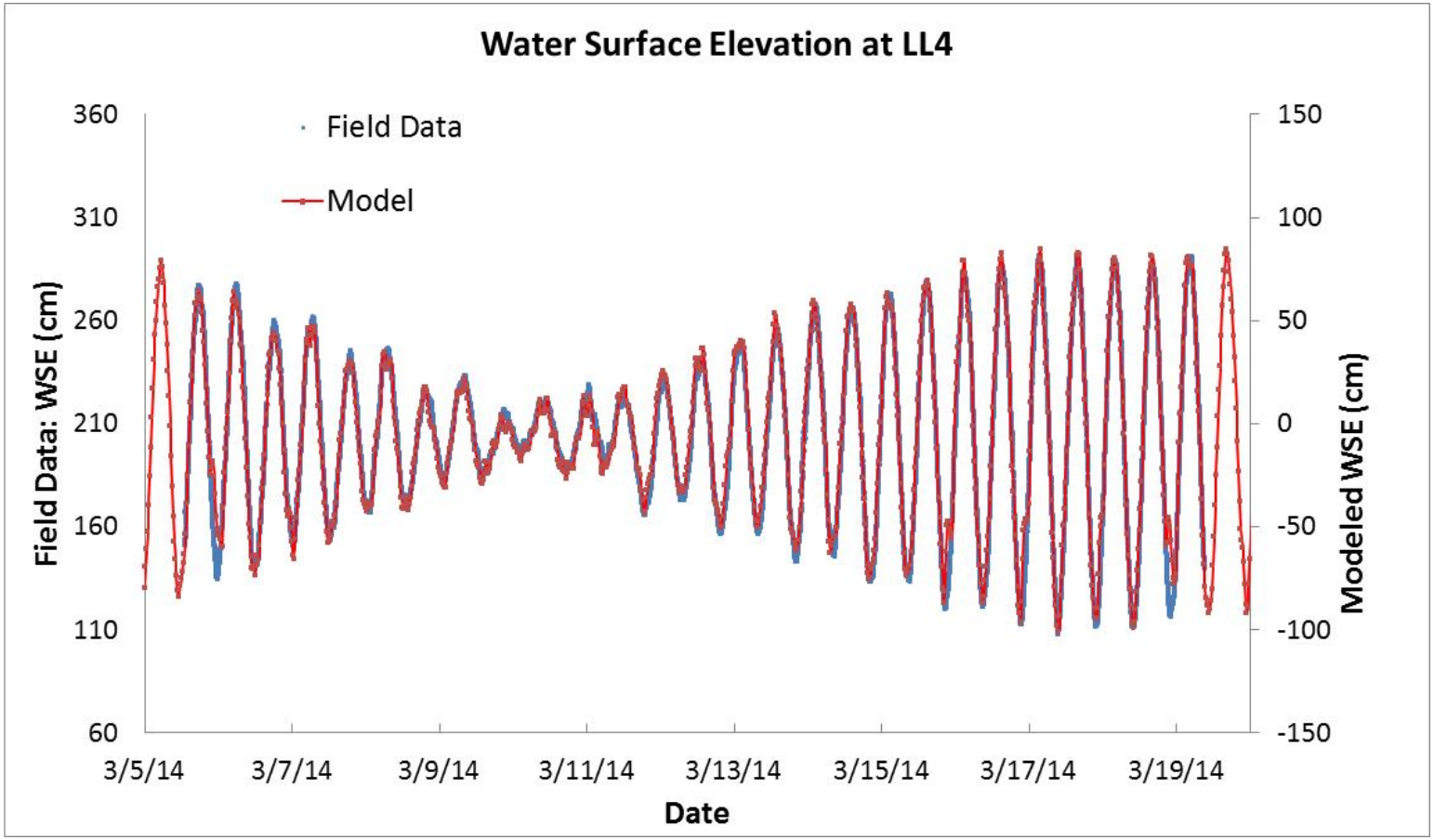

Figure 12. Simulated and measured water surface elevation at LL4 (30-min averaged). Field data were measured relative to the bottom while modeled data were measured relative to mean sea level.

4.2 CURRENTS

Currents were measured at five locations by upward-looking ADCPs. Measured currents were processed and averaged into three layers of the water column: the bottom layer, the mid-layer, and the surface layer. Results of mid-layer current components in the east (u) and north (v) were compared between the model and the measurements and shown in Figure 13 through Figure 17. Similar to the water level data, the 1-min data collected by the ADCPs were time-averaged more than 30 min for the comparison between measurements and model predictions.

Figure 13 and 14 show that simulated and measured current u and v components are in the same range at ADCP1 for both ADCP2 stations. Currents at ADCP2 were weaker (~ 10 cm/s) than those observed or modeled at ADCP1 throughout the period. Measured currents at ADCP2 before 10 March 2014 seem to be erroneous, and therefore were not included here. From 11–18 March 2014, measured and model-simulated currents at ADCP1 compare well for both u- and v-component, with current amplitudes fluctuating below 50 cm/s. Currents at ADCP3 station were up to ~ 50 cm/s, comparable to those at ADCP1, and considerably stronger than the currents at ADCP2, ADCP4, and ADCP5. The model simulated the current magnitude reasonably well. Currents at ADCP4 and ADCP5 stations were weak compared to those in the other regions. Both simulated and measured mean currents were ~ 5 cm/s.

Table 4 shows the statistics of the mean current amplitudes during the 4–18 March 2014 period. On average, mean amplitudes of the simulated currents compare fairly well with the measurements for all five ADCP stations. The largest model–data difference of the mean current amplitude is about -35% for ADCP2, followed by -24.4% at ADCP5, 17.2% for ADCP3, 16.4% for ADCP1, and -13.9% for ADCP4. Positive difference means field data is larger than model result, and conversely for negative. It should be noted that the mean tidal currents are the primary force that drive the long-term transport characteristics of the lagoon water, such as the flushing time.

Both measured and model-simulated currents show some variations of current amplitude in the water column, weakest current in the bottom layer, followed by mid-layer and currents in the surface is the strongest. When water-column current is vertically averaged, the average current amplitude is close to the current measured or simulated in the mid-layer. Therefore, for convenience, the SSC Pacific research team used mid-layer current for analysis and comparison between model and measurements.

Table 4. Model–data comparison of current at mid-water column at the four locations (5–19 March 2014).

Level Location	**Mean Current Amplitude at Mid-Water Column (cm/s)**		**Difference (Field Fata-Model)/Model (%)**
	Model	**Field Data**	
ADCP1	10.2	12.2	16.4
ADCP2	5.4	4.0	-35.0
ADCP3	10.1	12.2	17.2
ADCP4	4.9	4.3	-13.9
ADCP5	5.1	4.1	-24.4

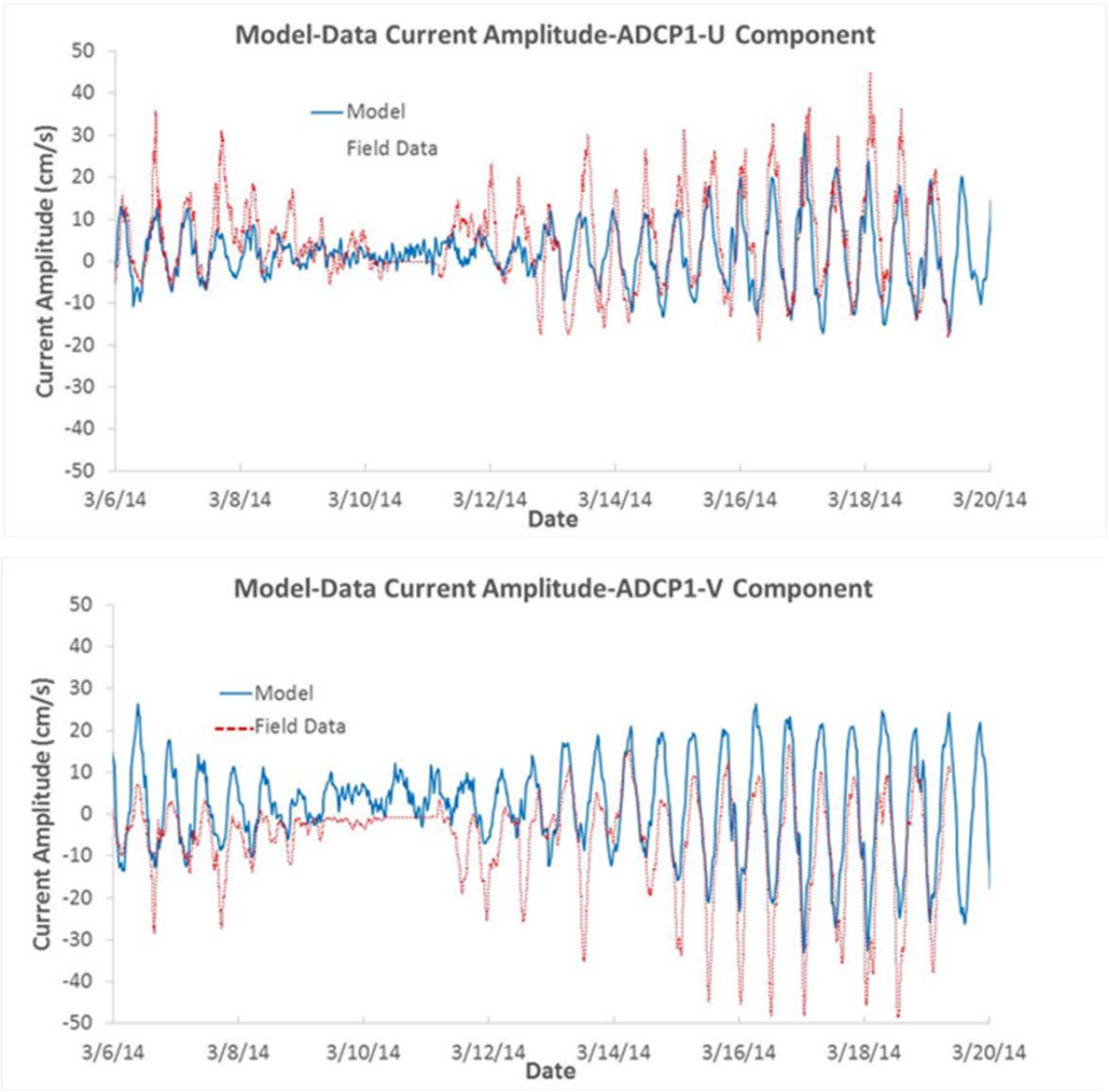

Figure 13. Model–data comparison of current velocity in east direction (U) and north (V) direction at ADCP1.

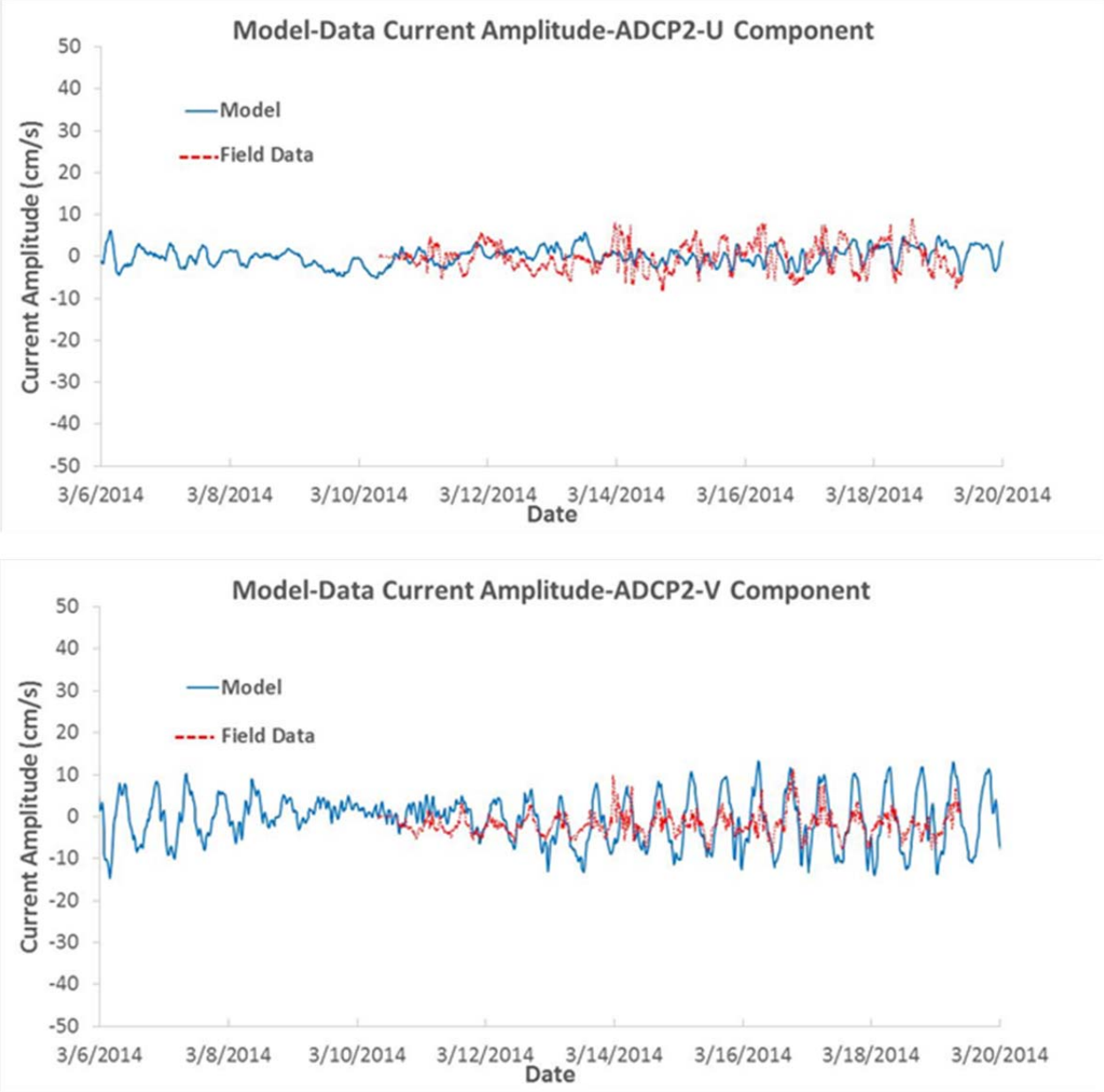

Figure 14. Model–data comparison of current velocity in east direction (U) and north (V) direction at ADCP2.

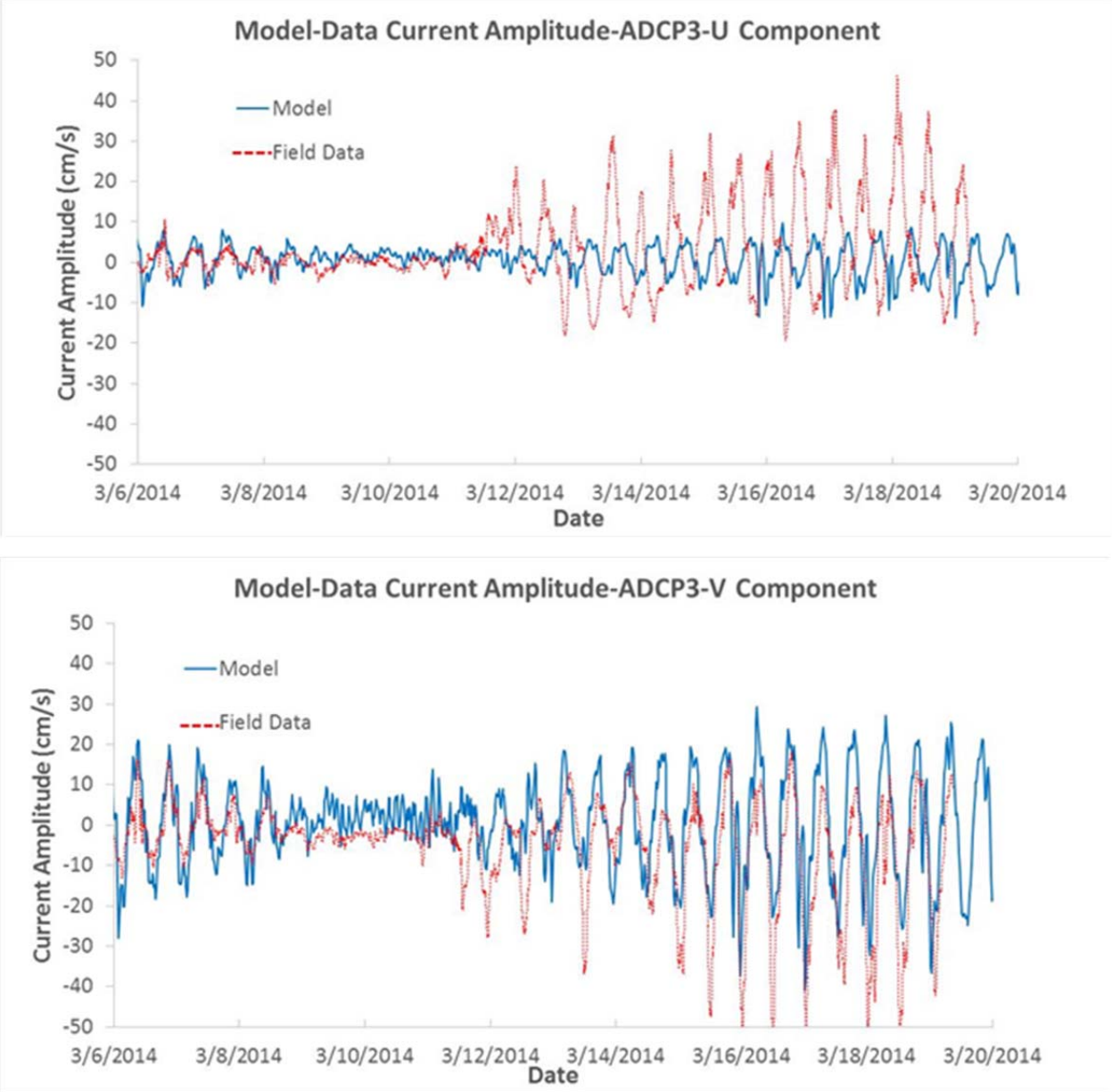

Figure 15. Model–data comparison of current velocity in east direction (U) and north (V) direction at ADCP3.

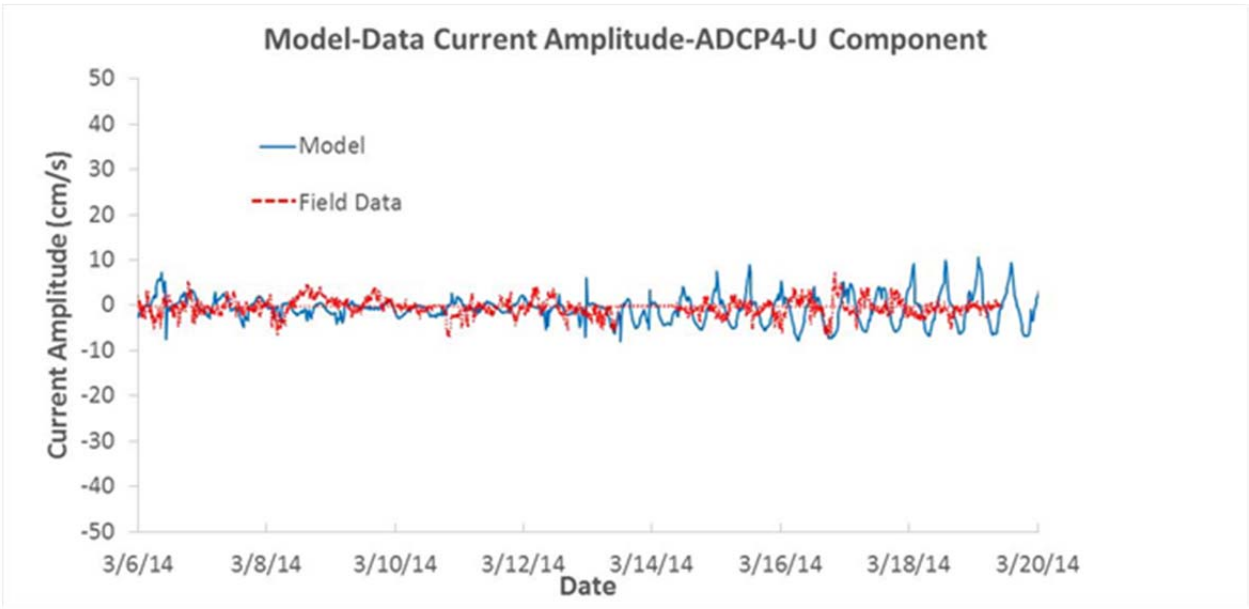

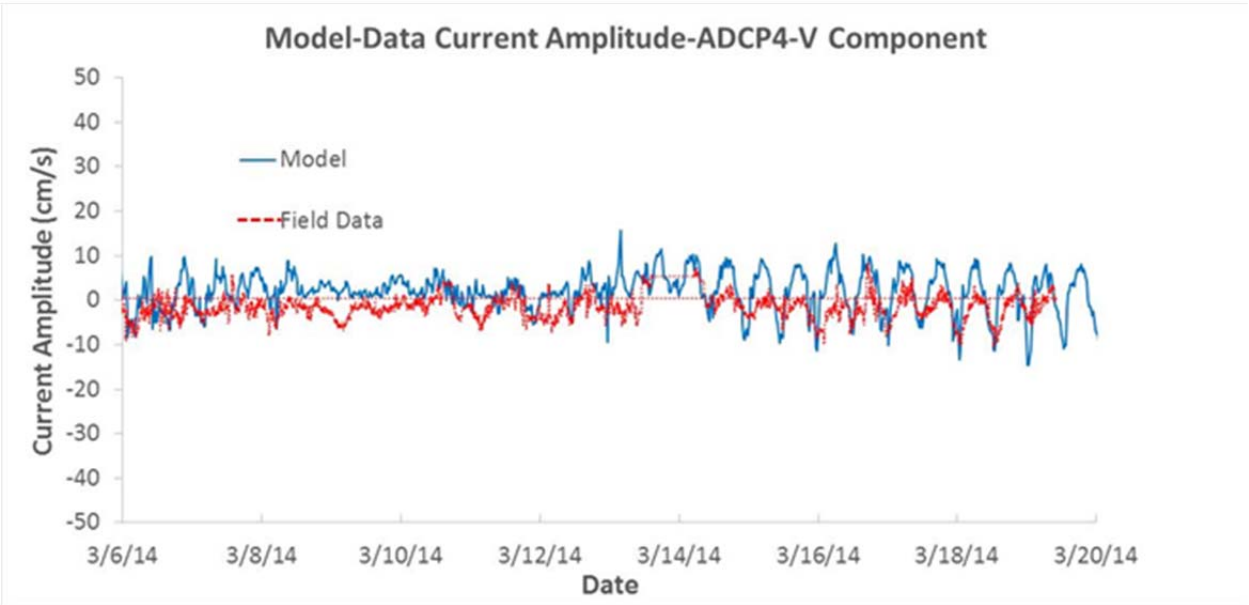

Figure 16. Model–data comparison of current velocity in east direction (U) and north (V) direction at ADCP4.

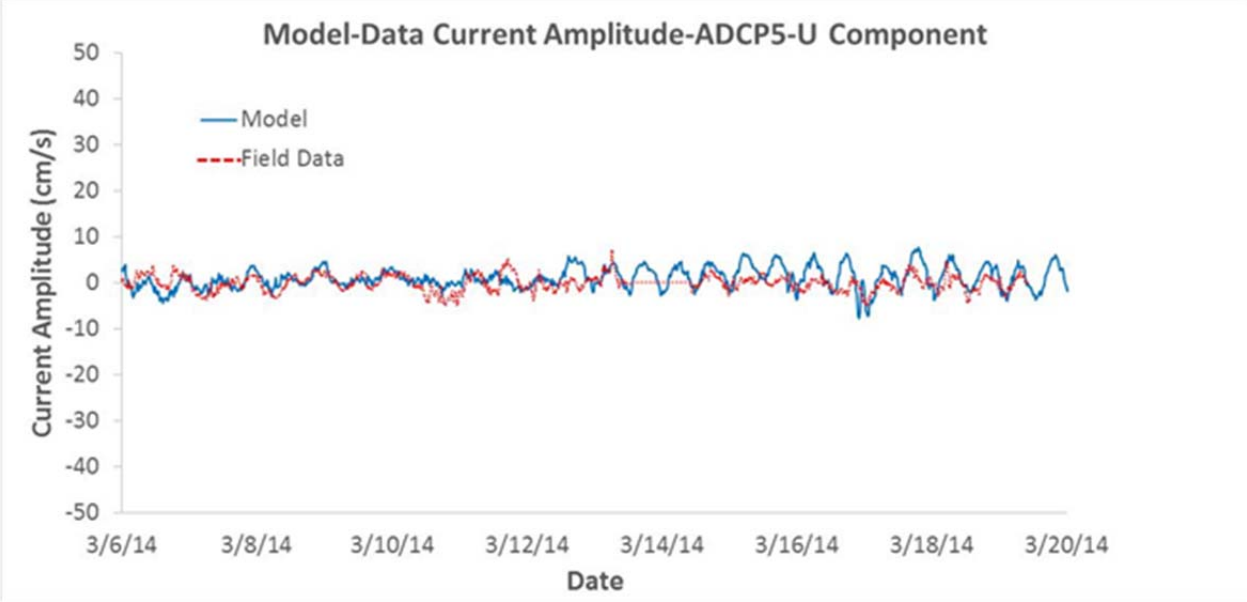

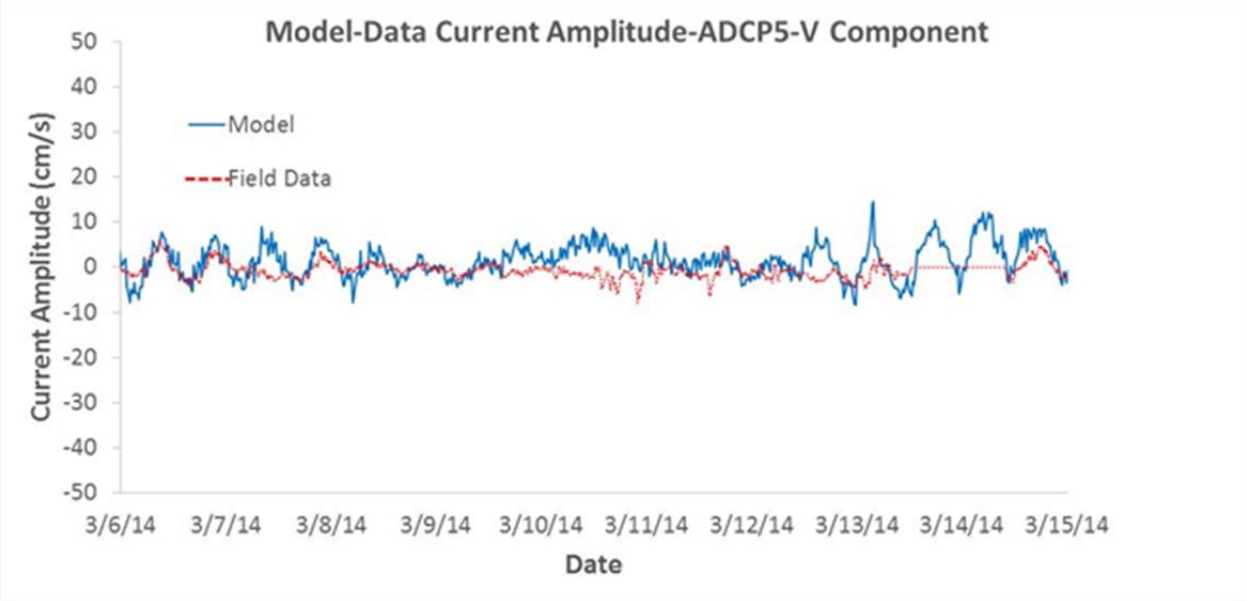

Figure 17. Model–data comparison of current velocity in east direction (U) and north (V) direction at ADCP5.

4.3 FLUSHING TIME

Flushing time in the Diego Garcia Lagoon was calculated directly from the EFDC model. The Lagoon is divided into four different regions and the overall lagoon region (Figure 19). To simulate flushing characteristics in any one of the five regions (four sub-regions and the oval lagoon), A tracer with an initial condition of 100 mg/L was assigned to each model grid cell within that region, keeping all the other cells and boundary conditions as zero. As the EFDC hydrodynamic simulation starts, the initial tracer concentration within the regions was dispersed, transported, and flushed out of the lagoon. The total mass of the tracer within the lagoon was calculated as percentages of the initial total mass throughout the simulation period (Figure 20). Flushing time can be defined and chosen as the time when 90 or 95% of the total initial mass is flushed out of the lagoon.

Table 5 shows the results of the flushing time calculated as 10 and 5% of the initial mass remaining in the region, which correspond to 90 and 95%, respectively, of the initial mass flushed out of the region. It shows that flushing time generally is the longest in Region 1 (southernmost part of the lagoon) and decreases toward the mouth. Flushing time in Region 1 (southernmost part of the lagoon) is about 38 to 43 days (10 to 5% initial mass remaining), decreasing to 34 to 41 days for Region 2, 22 to 28 days for Region 3, and to 19 to 25 days for Region 4, which is closest to the ocean mouth. If the lagoon is considered as one single water body, the flushing time is estimated to be 24 to 32 days, approximately in between Regions 1 and 2 and Regions 3 and 4.

Table 5. Flushing times for different regions predicted by EFDC model.

	Time for 90% of Initial Mass Flushed Out of Lagoon (days)	Time for 95% of Initial Mass Flushed Out of Lagoon (days)
Region 1	38	43
Region 2	33	41
Region 3	22	28
Region 4	19	25
Entire Lagoon	24	32

4.4 STRATIFICATION

The potential effects of stratification on flushing of the lagoon were evaluated based on the field data and modeling simulations. Vertical profiles from the four CTD surveys were compiled and gridded along the axis of the lagoon to construct sections of salinity, temperature, and density. The first survey conducted on 6 March 2014 included 24 stations along the axis of the lagoon. The survey was repeated on 11 March 2014, 13 March 2014, and 18 March 2014, with a total of 6, 7, and 7 profile locations, respectively. While the data for these later surveys were sparser, the gridded axial sections still provided a reasonable description of the salinity, temperature, and density distributions in the lagoon.

Results from the CTD surveys are shown in Figure 20 through Figure 22. Salinity distributions for the four surveys showed similar patterns, with highest salinities near the mouth of the lagoon and lowest salinities near the head. Vertical stratification of salinity tended to be strongest in the inner half of the lagoon, while the outer portion of the lagoon was generally more vertically mixed. Salinities generally ranged from a low of about 36 psu at the head, to a high of about 38 psu near the mouth, although surface salinities in Turtle Cove at the head of the lagoon were measured as low as 19 psu. In general, these conditions are consistent with a weak, partially mixed estuarine system.

Temperature distributions for the four surveys also showed similar patterns, with cooler water near the mouth of the lagoon, and warmer water near the head. Vertical stratification of temperature was generally lacking. Temperatures generally ranged from a low of about 28 to 29 ˚C near the mouth to a high of about 30 to 31 ˚C at the head. The surveys on 11 March 2014 and 13 March 2014 showed somewhat warmer conditions throughout the lagoon in comparison to the 6 March 2014 and 18 March 2014 surveys. The distributions suggest that the inner lagoon waters tend to warm by about 2 ˚C above the adjacent ocean waters due to the residence time of the lagoon and the isolation of these waters from cooler ocean waters at depth.

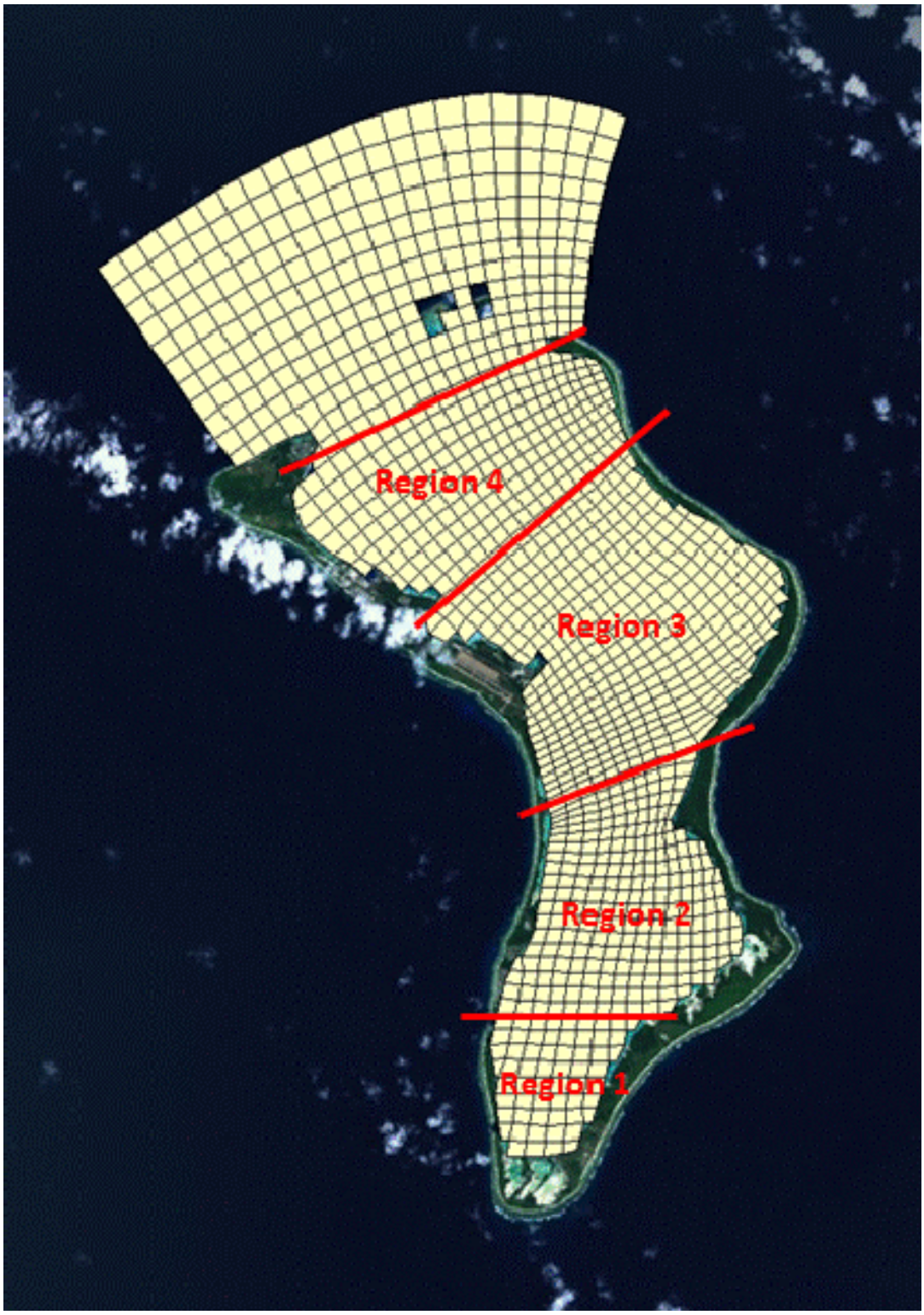

Figure 18. Overall Diego Garcia Lagoon and four regions for flushing time calculations. Image © 2014 Google DigitalGlobe, Data SIO, NOAA, U.S. Navy, NGA, GEBCO.

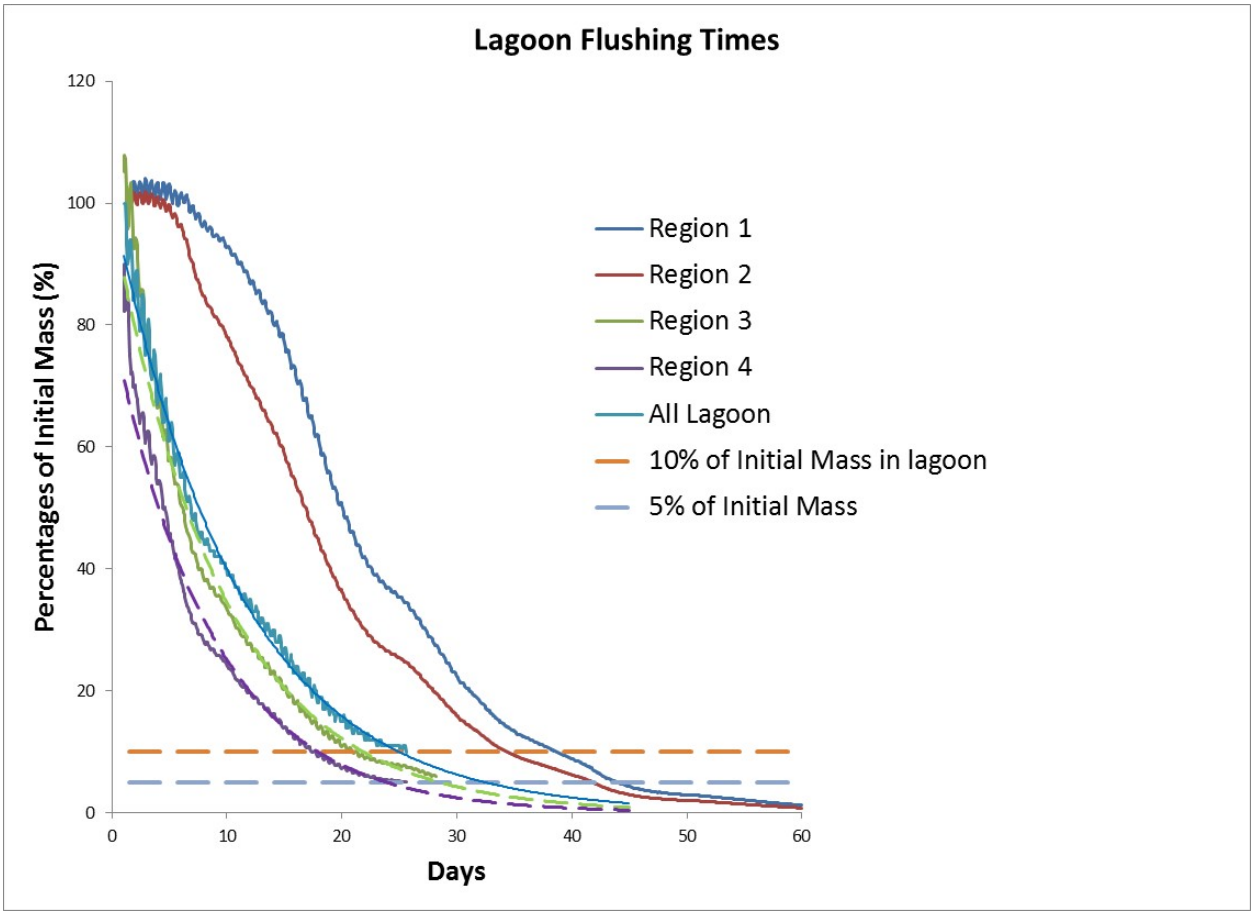

Figure 19. Total mass remaining in the specific water body regions.

Density distributions for the four surveys were developed from the temperature and salinity data and calculated as the density anomaly $\sigma = \rho\text{-}1000$, where ρ is the density in kg/m^3. Density variations tended to be dominated by salinity as opposed to temperature, and thus the density distributions followed similar patterns to that of salinity. Highest densities were near the mouth of the lagoon, and lowest densities were in the surface waters near the head. Vertical stratification was most significant in the inner portion of the lagoon, with weaker stratification in the outer portion of the lagoon toward the mouth. Density anomaly ranged from a high of about 24 at the mouth to 22 at the head. The survey on 13 March 2014 showed the strongest vertical stratification throughout the lagoon, but a limited number of vertical profiles existed, especially in the outer lagoon.

The strength of the vertical stratification in estuaries is often characterized by the stratification parameter of Hansen and Rattray (1966), which is calculated as the ratio of the top-to-bottom salinity difference, ∂S, to the mean salinity over an estuarine cross section, S_0. For systems with strong stratification, $\partial S/S_0$ tends toward a value of 1, while for weak stratification, the ratio tends toward zero. Figure 23 illustrates the stratification conditions along the axis of the lagoon. On average, the stratification parameter is in the range of 0.01 throughout most of the lagoon, except the inner lagoon beyond about 22 km, where it increases to about 0.1. Thus, stratification in the lagoon during the period of the surveys would be characterized as relatively weak except in the farthest inner portion of the lagoon, where it was moderate. This is consistent with the characterization of the lagoon as a weak, partially mixed estuary.

Results of the EFDC model simulations were compared with field data for salinity and temperature during the four surveys, as shown in Figure 24 and Figure 25, respectively. The general patterns of simulated salinity are similar to those recorded by the field data, with highest salinities near the mouth of the lagoon and lowest salinities near the head. Simulated salinity in the outer portion of the lagoon also reflects the vertically mixed characteristics of the region, which was also observed in the field data. Compared to field data, simulated salinity shows stronger influence of freshwater inflows from the head of the lagoon, pushing the lower salinity further out into the middle and outer portions of the lagoon. This results in 0.1- to 0.5-psu difference in salinity in the middle portion of the lagoon. Further model refinement could reduce this difference by reducing the freshwater inflows to the lagoon, but the results were deemed sufficiently consistent with the field data to evaluate flushing time.

Simulated temperature (Figure 25) compares well with the field data (Figure 21) in both lateral gradients and vertical stratification (weak) for all four surveys. Temperature in the lagoon was primarily governed by the water temperature from the two boundaries from the ocean and the freshwater inflows from the head of the lagoon. Another important boundary input was the ambient weather input through the water surface, which included solar radiation, air temperature, relative humidity, precipitation, evaporation, and cloud cover. Compared to field data, simulated temperature shows stronger stratification in the water column. But the difference in temperature stratification, with a difference of less than 0.5 ˚C between model and field data, is small, which does not change the vertically mixed characteristics of the outer lagoon water.

The model results were used to calculate the stratification parameter of Hansen and Rattray (1966) for comparison to the field measurements. On average, the modeled stratification parameter was in the range of 0.01 throughout most of the lagoon, comparable to the field data except the inner lagoon beyond about 22 km, where the field data indicated stronger stratification than the model.

Overall, simulated and measured water temperature, salinity, and stratification were in good agreement between the model and the field data for all the four surveys.

4.5 VERTICAL MIXING CHARACTERISTICS

The EFDC model was used to simulate and evaluate the vertical mixing characteristics of the outer portion of the lagoon. Since ship discharges are generally limited to the surface water layer, simulations were conducted with discharge to the surface layer.

The water column was equally divided into five layers, with the thickness of each layer fluctuating with the changing water depth during the simulation. Tracer (neutrally buoyant dissolved substance) was added to the surface layer at the selected locations (Figure 26 and Figure 27). Total mass at the surface layer and bottom layer were recorded during the simulation as percentages of the total mass added.

4.5.1 Surface Discharge and Water Column Mixing

Two surface discharge scenarios were simulated. In the first scenario, the tracer was discharged to each of the surface layer grid cells (Figure 27) at a rate of 1 kg/sec over 24 hours from Day 1.5 to Day 2.5. Simulation continues for 6.5 days, which showed that while vertical mixing continues, it is highlighted by the evolution of the total mass in the surface layer and the bottom layer. Figure 28 shows that once the addition of tracer ceased at Day 2.5, total mass in the surface started its decreasing trend, loosing mass by mixing to the deeper water, whereas total mass in the bottom layer started to increase simultaneously. At Day 4.5, two days after addition of tracer ceases, total tracer mass at the surface layer is at the same level as that at the bottom layer, reflecting a vertical mixing.

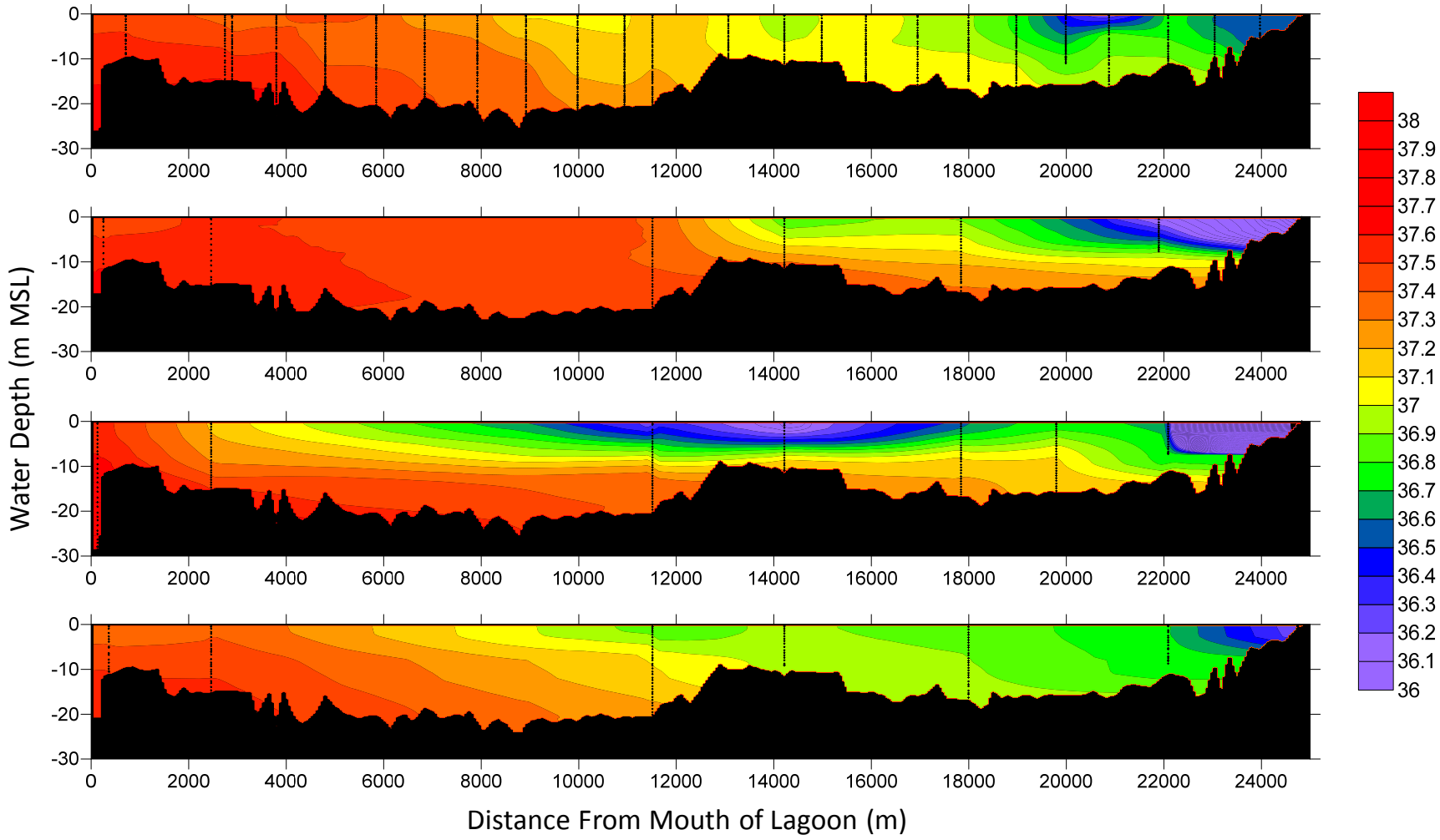

Figure 20. Axial distribution of salinity (psu) in Diego Garcia Lagoon based on the four vertical profile surveys. Black dots indicate locations of measurements. The mouth of the lagoon is on the left and the head of the lagoon is on the right.

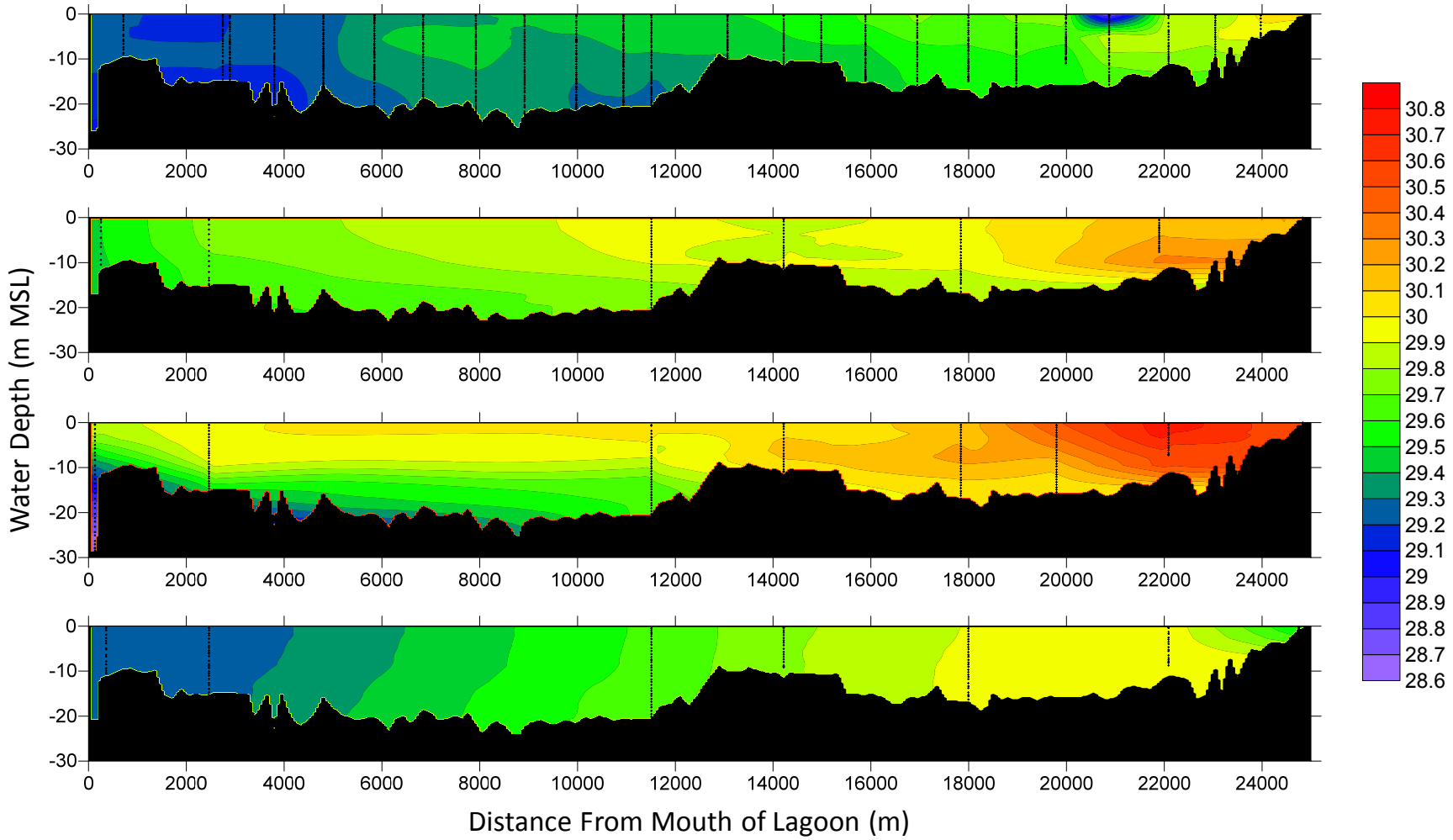

Figure 21. Axial distribution of temperature (C) in Diego Garcia Lagoon based on the four vertical profile surveys. Black dots indicate locations of measurements. The mouth of the lagoon is on the left and the head of the lagoon is on the right.

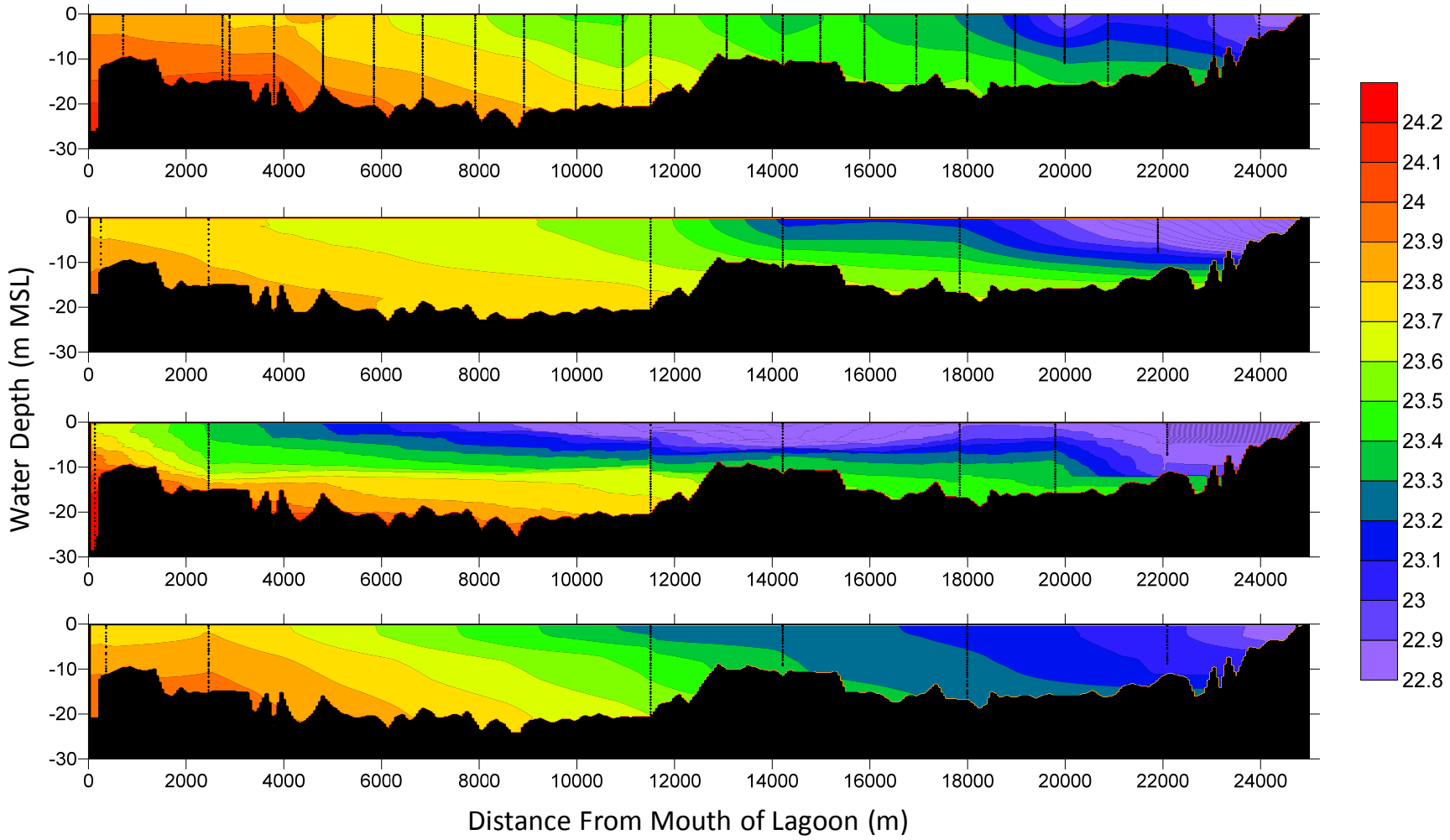

Figure 22. Axial distribution of the density anomaly in Diego Garcia Lagoon based on the four vertical profile surveys. Black dots indicate locations of measurements. The mouth of the lagoon is on the left and the head of the lagoon is on the right.

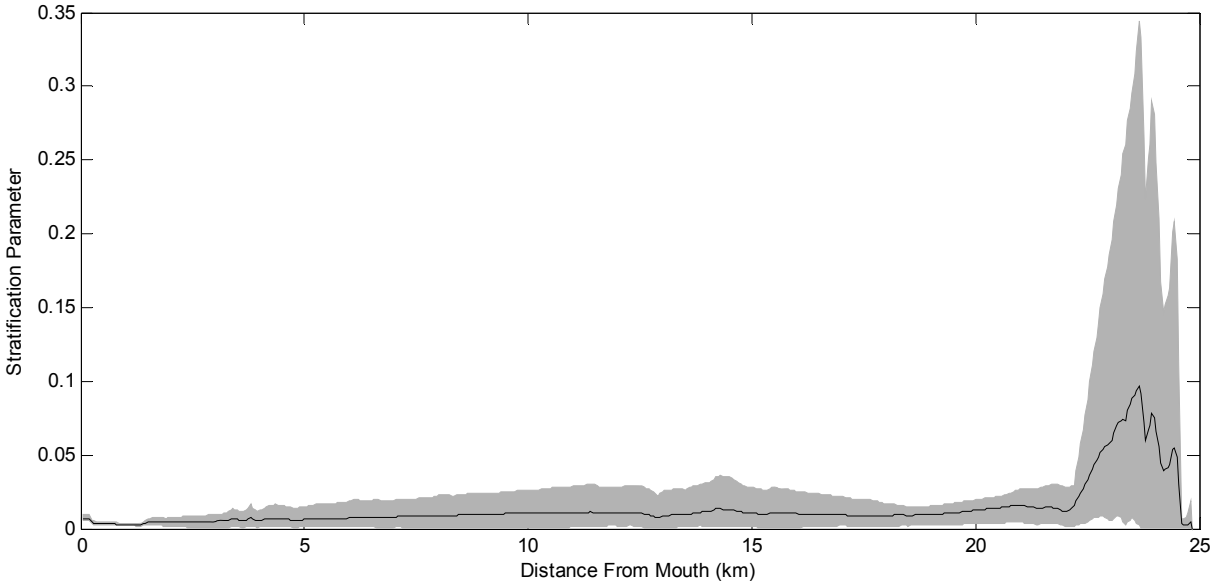

Figure 23. Stratification parameter for Diego Garcia Lagoon as a function of distance from the mouth. The grey shaded area represents the range from the four surveys, while the black line represents the mean of the four surveys.

At this vertical mixing condition, both tracer mass at the surface and the bottom layers are at about 3.5% of the total added mass from the discharge, meaning that only 3.5% of the total discharge mass ended up in the bottom layer (and the surface layer).

In the second scenario, tracer discharges took place at the rate of 1 kg/s to the same locations (Figure 27) during the three consecutive slack high tides (Day 1.375 to 1.406, Day 1.885 to 1.917, and Day 2.396 to 2.427). Figure 29 shows that the evolution of total mass between the surface layer and the bottom layer is very similar to that for the continuous discharge scenario. At Day 4.5, two days after addition of tracer ceases, both tracer mass at the surface and the bottom layers are at about 2.4% of the total added mass from the discharge, which is lower than the continuous discharge scenario by a difference of 1% of total added mass.

To understand vertical mixing in the outer portion of the lagoon, a simulation was conducted by assigning an initial concentration of tracer at the same locations (Figure 27) at Day 1.125. Figure 30 through Figure 34 show simulated tracer concentration contours at every 12 hours after Day 1.125 (t = 0). During the first 24 hours, tracer in the surface layer started to transport to other regions and lose mass to the lower layers, whereas concentrations in the bottom layer started to increase. At Day 3.125 (2 days after the initial condition), tracer concentrations in the surface layer and bottom layer are at about the same level, which is consistent with the vertical mixing discussion made previously. In the six sets of figures, tracer concentration spectrum for the initial condition (Figure 30) is 10 times the spectra for the subsequent five tracer concentration contours during the first 2.5 days.

Since most ship discharges are directly to the surface water, it is necessary to know if this will impact the flushing time estimates in Section 4.3. Under the same scenario, two initial tracer release conditions were assigned, one at the water column and one at the surface layer only. The model simulated over 30 days and flushing times for both the water-column discharge and the surface layer discharge scenarios were estimated (Figure 35; Table 6). Flushing time for the continuous discharge scenario is estimated to be 19 and 28.5 days for 10 and 5% of the initial mass remaining in the

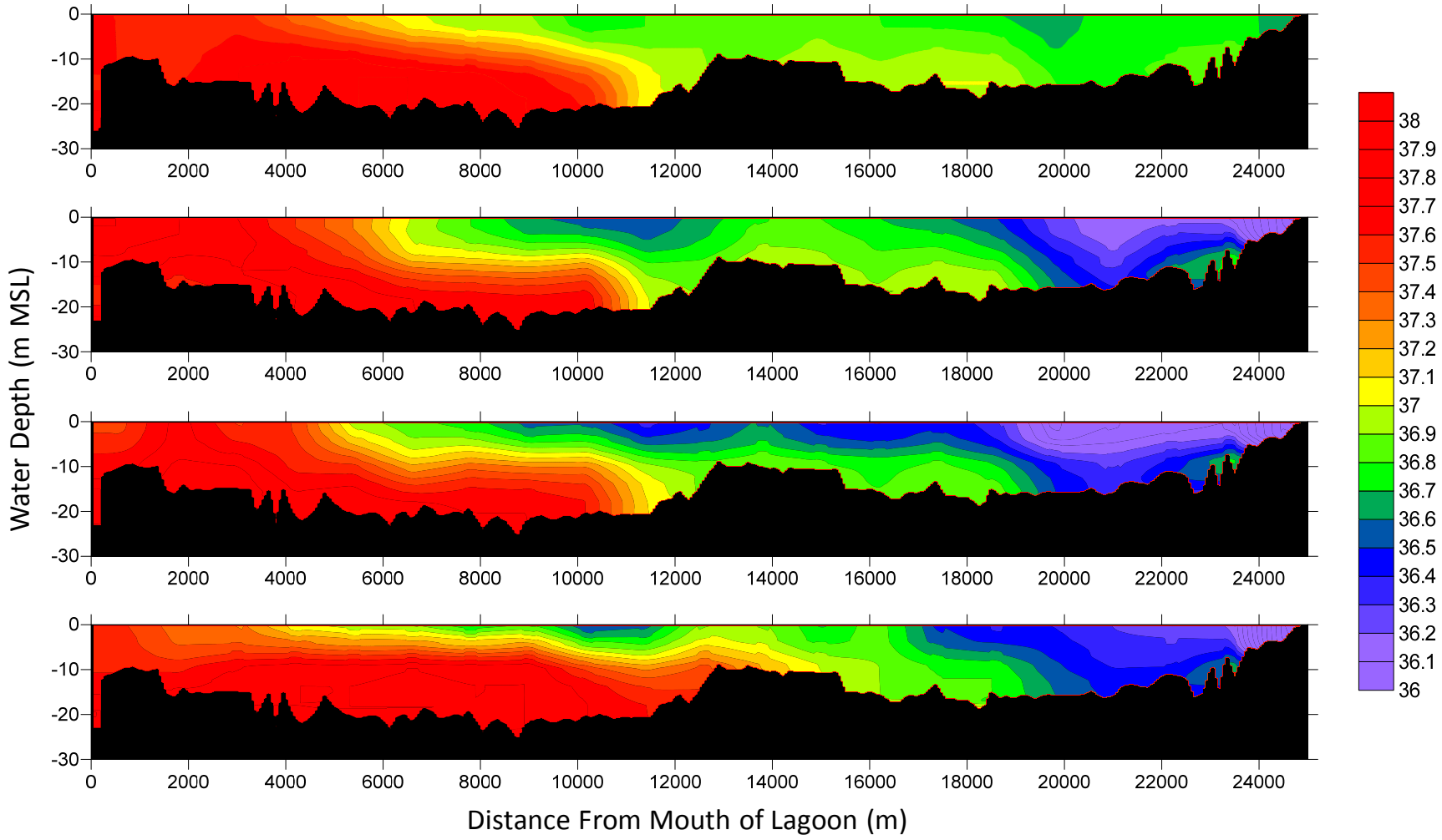

Figure 24. Axial distribution of salinity (psu) in Diego Garcia Lagoon based on model simulations for the same time periods as the four vertical profile surveys. The mouth of the lagoon is on the left and the head of the lagoon is on the right.

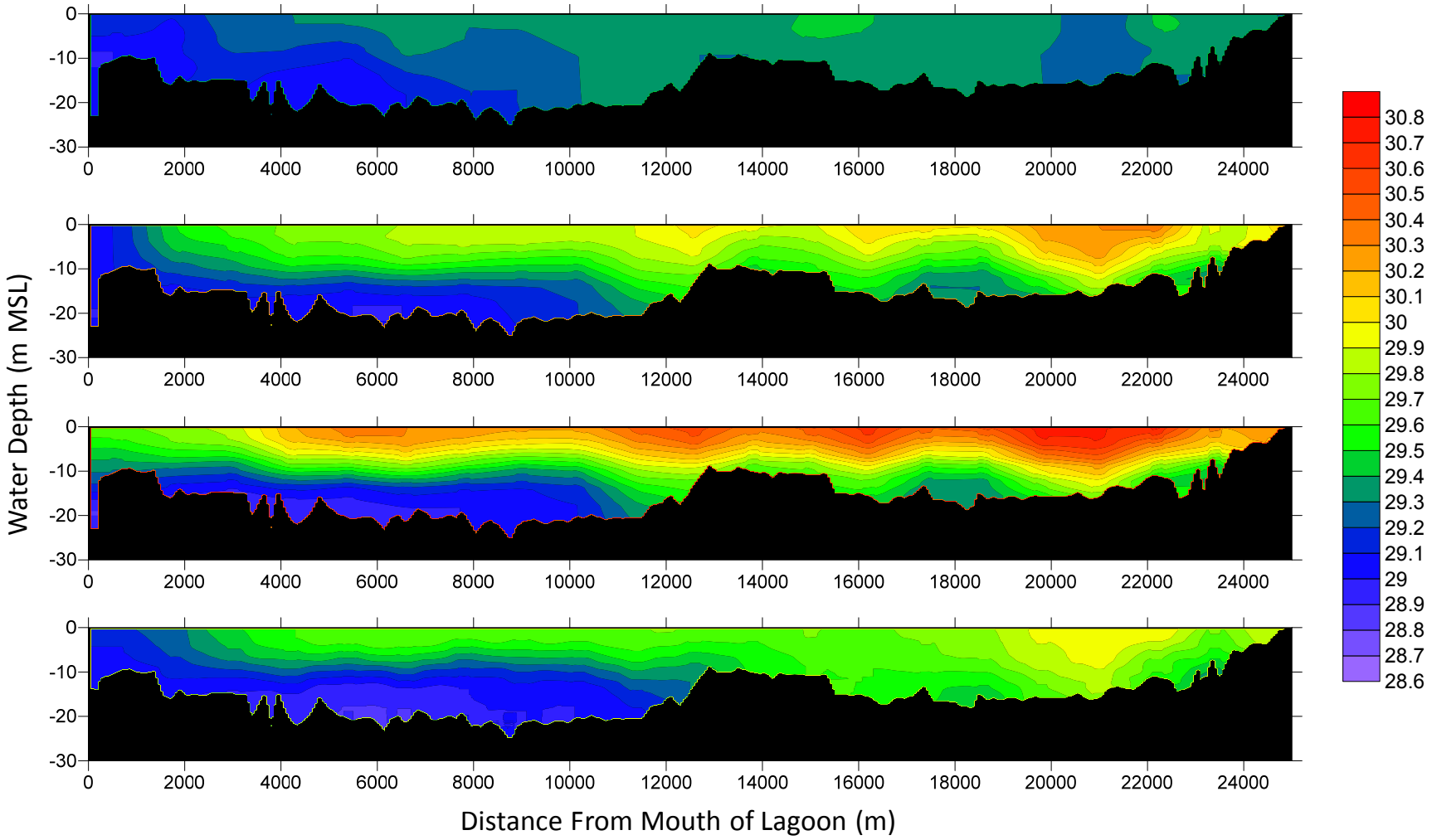

Figure 25. Axial distribution of temperature (C) in Diego Garcia Lagoon based on model simulations for the same time periods as the four vertical profile surveys. The mouth of the lagoon is on the left and the head of the lagoon is on the right.

lagoon, respectively. Flushing time for the surface discharge scenario is estimated to be 17.6 to 27 days, which is about 1.5 days shorter than those for the continuous discharge scenario.

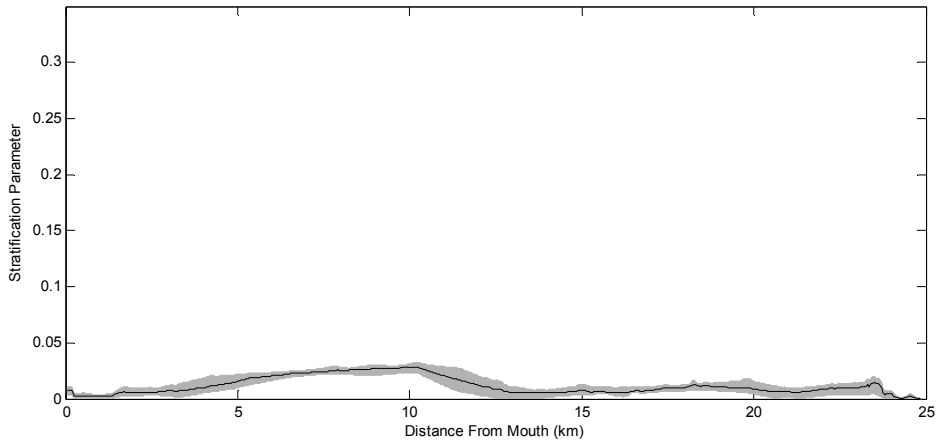

Figure 26. Stratification parameter for Diego Garcia Lagoon as a function of distance from the mouth based on the model results for salinity. The grey shaded area represents the range from the model results corresponding to the four field survey events, while the black line represents the mean of the four model results.

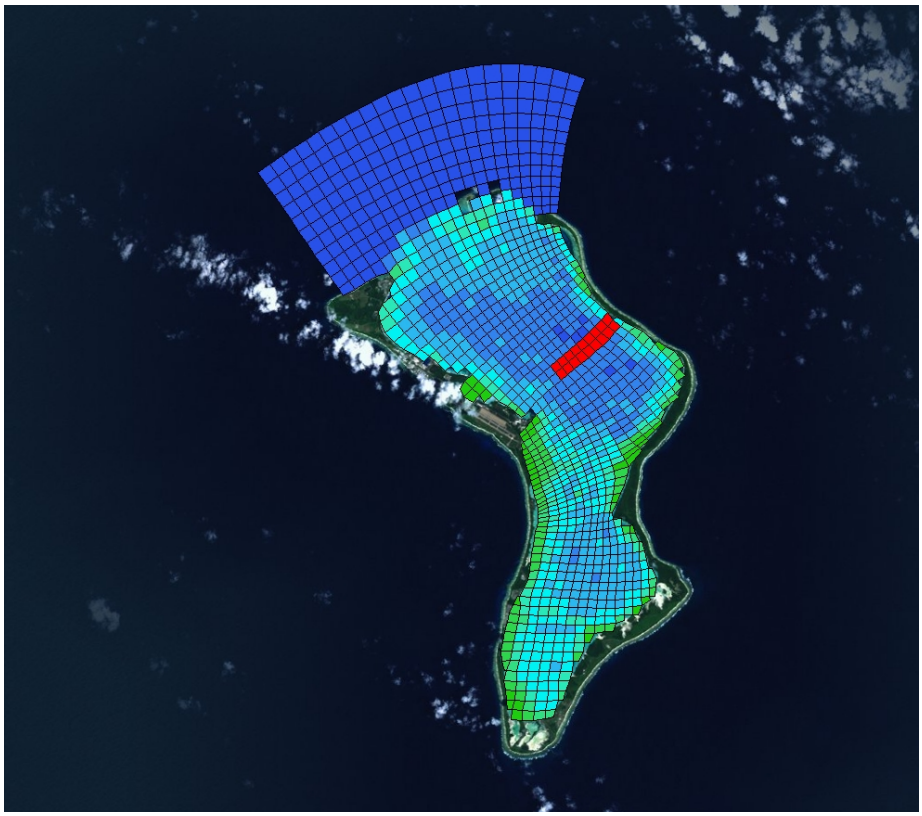

Figure 27. Locations of discharge (grid cells in red) for the vertical mixing characteristics modeling study. Image © 2014 Google DigitalGlobe, Data SIO, NOAA, U.S. Navy, NGA, GEBCO.

Table 6. Flushing times for water-column discharge and surface discharge by EFDC model.

	Time for 90% of Initial Mass Flushed Out of Lagoon (days)	Time For 95% of Initial Mass Flushed Out of Lagoon (days)
Discharge in water column	19	28.5
Discharge in surface layer	17.6	27

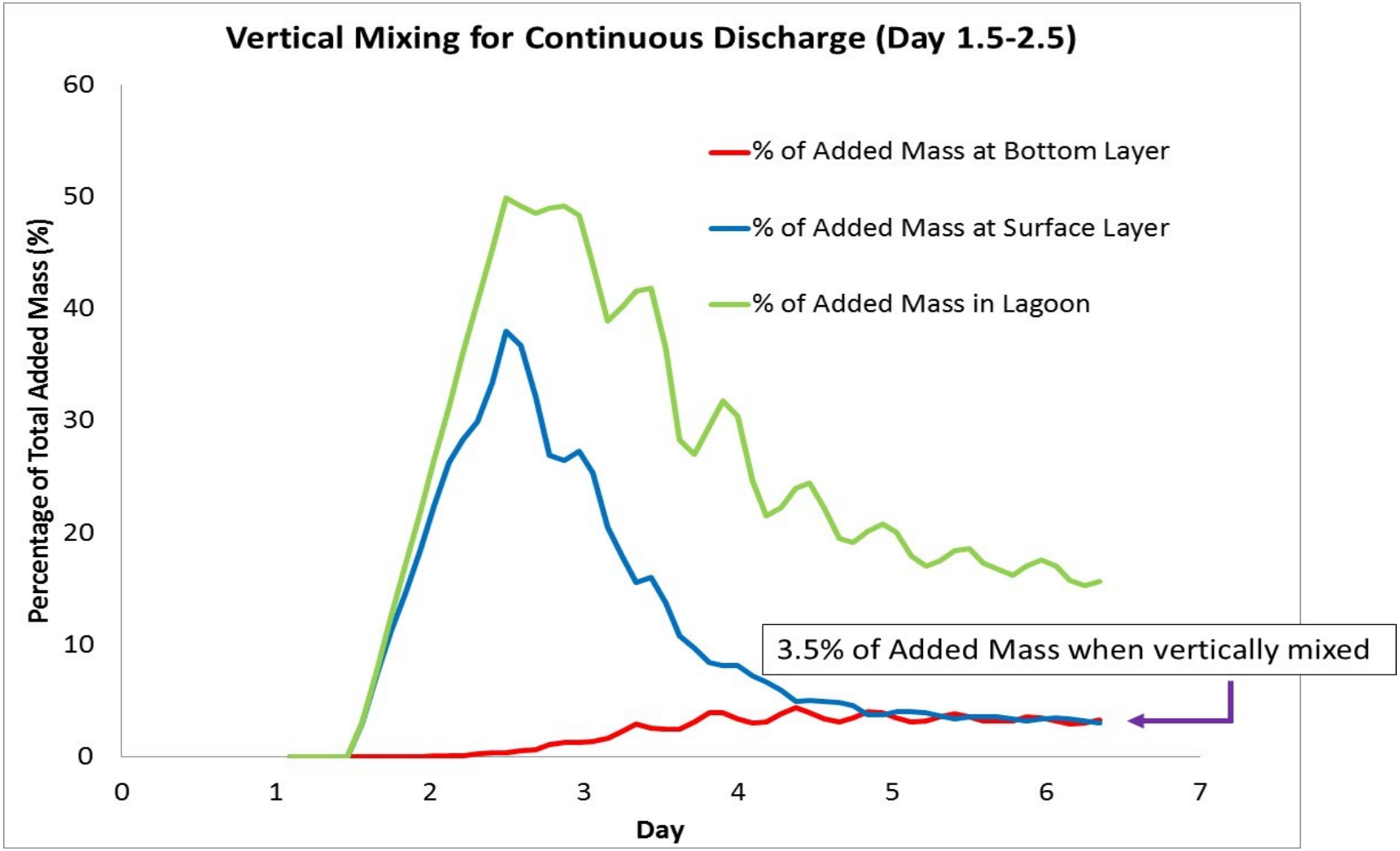

Figure 28. Time series of tracer mass for total tracer remaining in the lagoon surface layer and bottom layer, in percentages of total added mass discharged for the continuous discharge during Day 1.5 to 2.5.

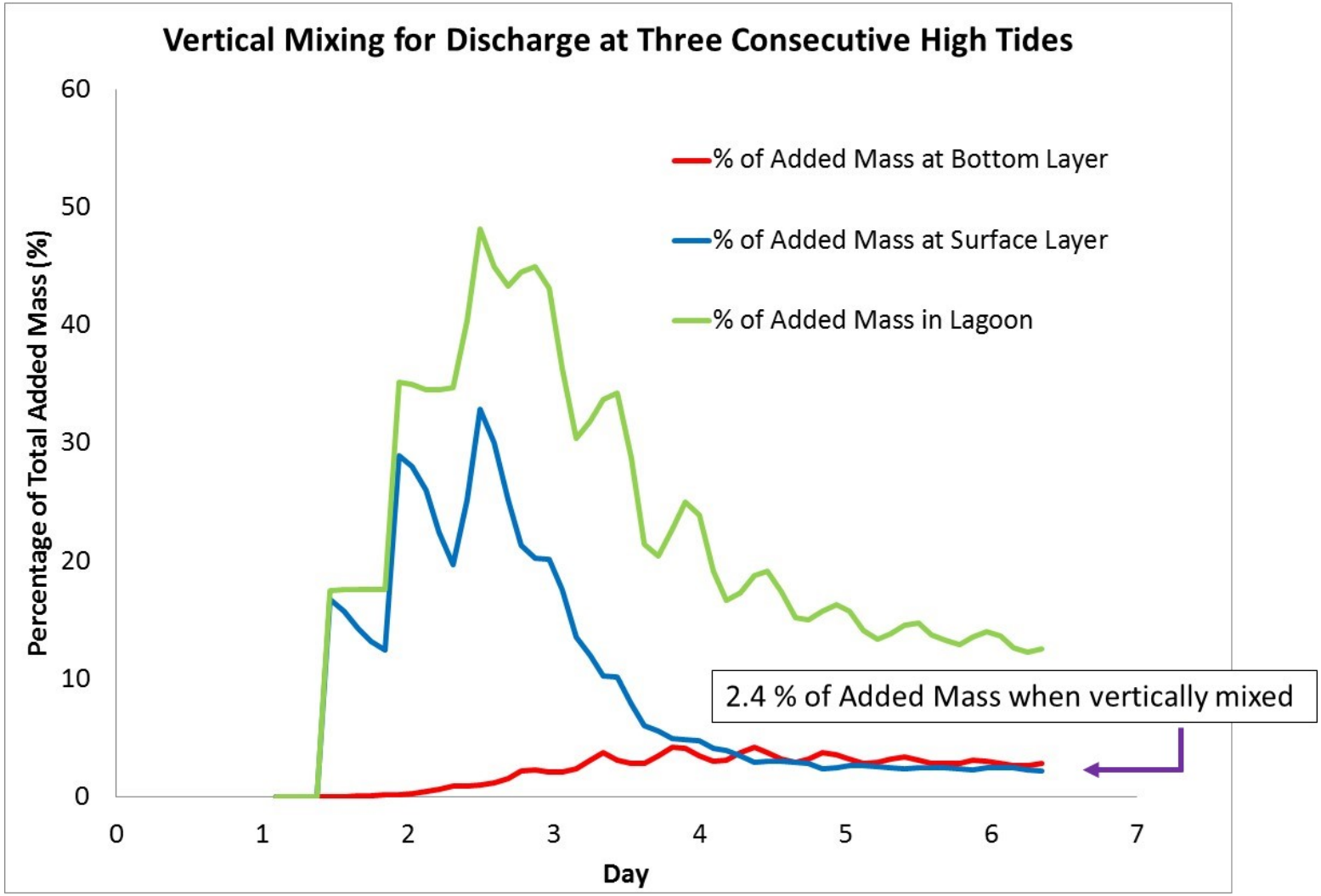

Figure 29. Time series of tracer mass for total tracer remaining in the lagoon surface layer and bottom layer, in percentages of total added mass discharged during three consecutive slack high tides during Day 1.375 to 2.427.

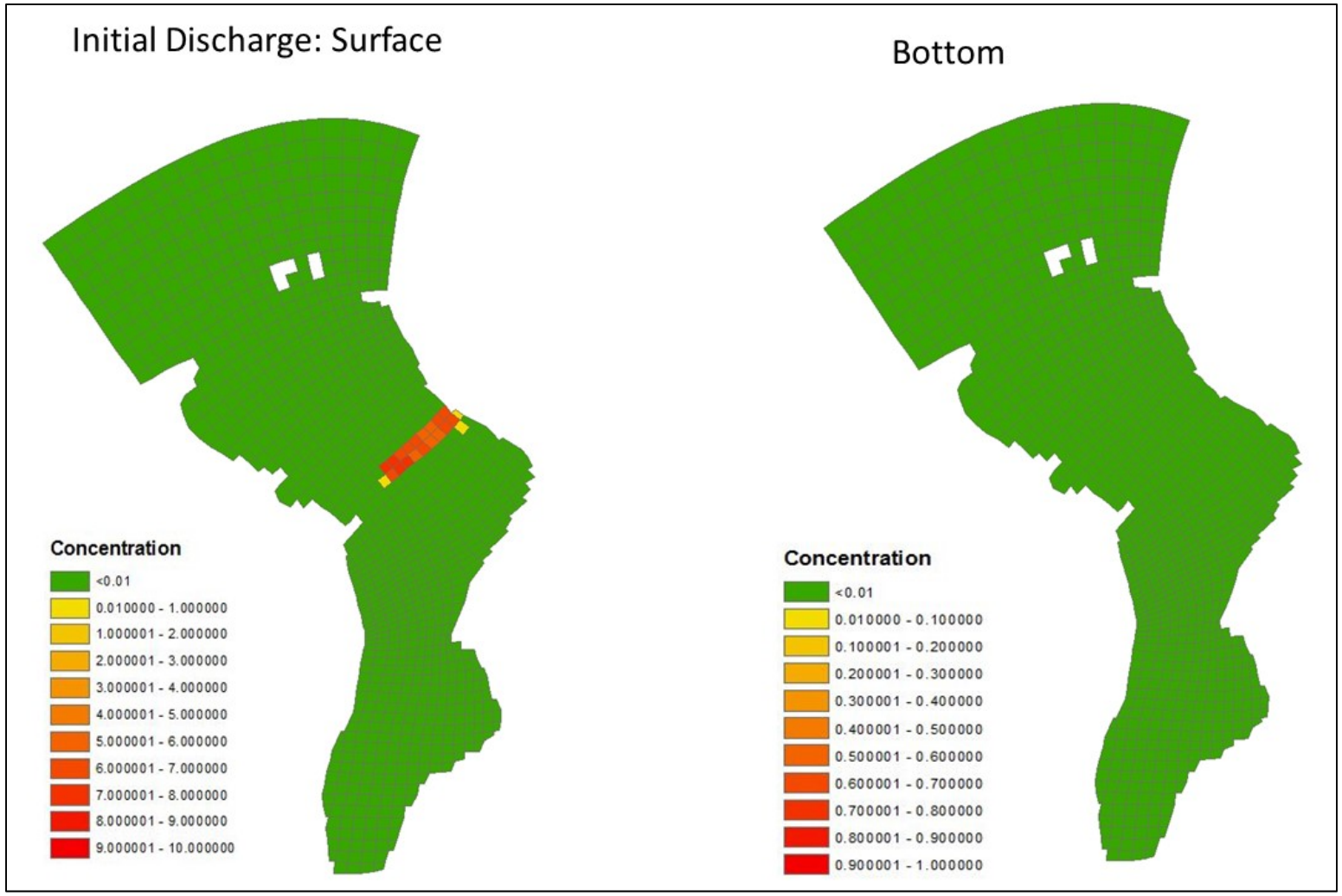

Figure 30. Tracer discharge and vertical mixing study: tracer concentrations in surface and bottom layer at the initial discharge condition (t = 0 hours).

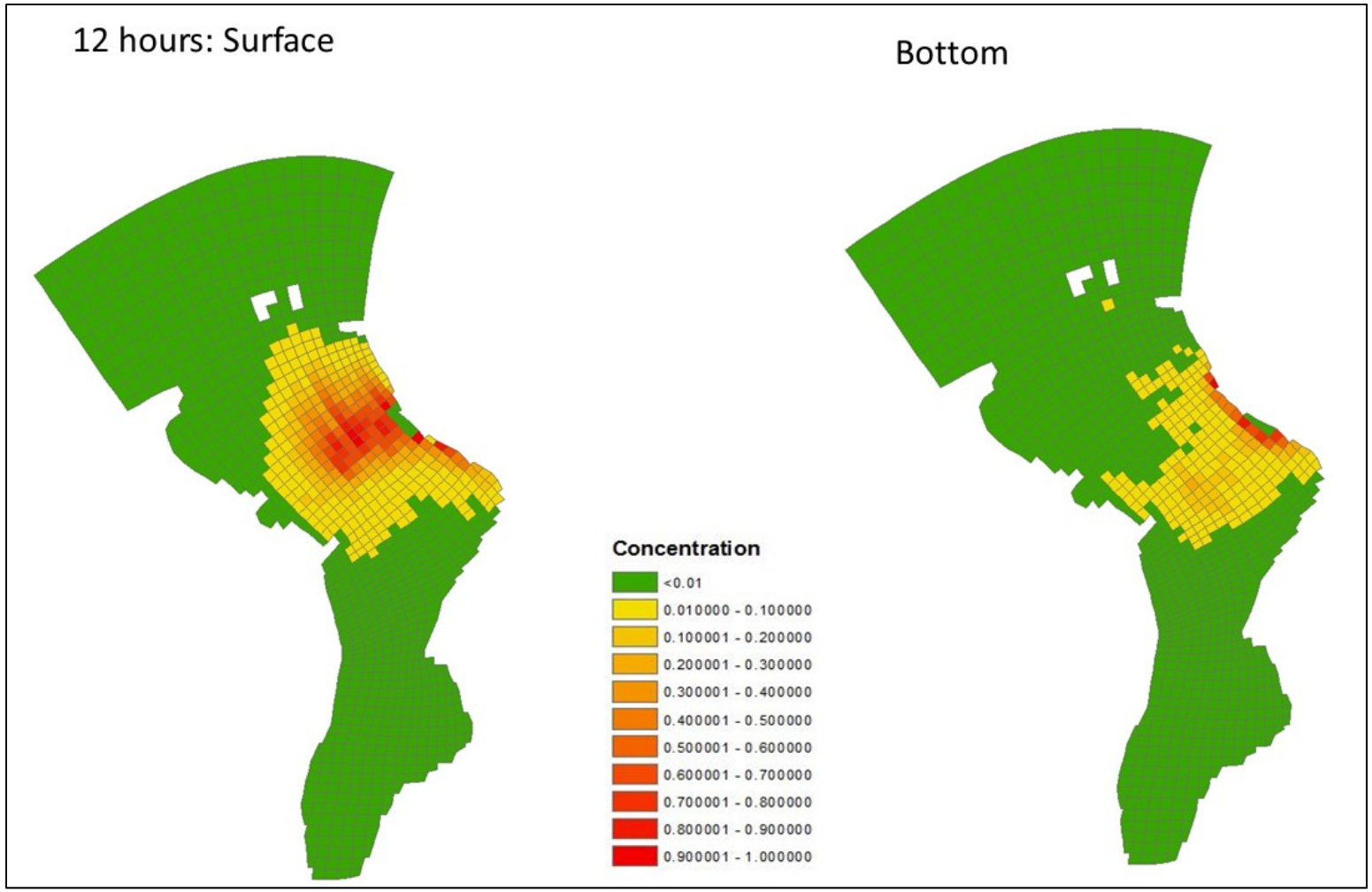

Figure 31. Tracer discharge and vertical mixing study: tracer concentrations in surface and bottom layer at 12 hours.

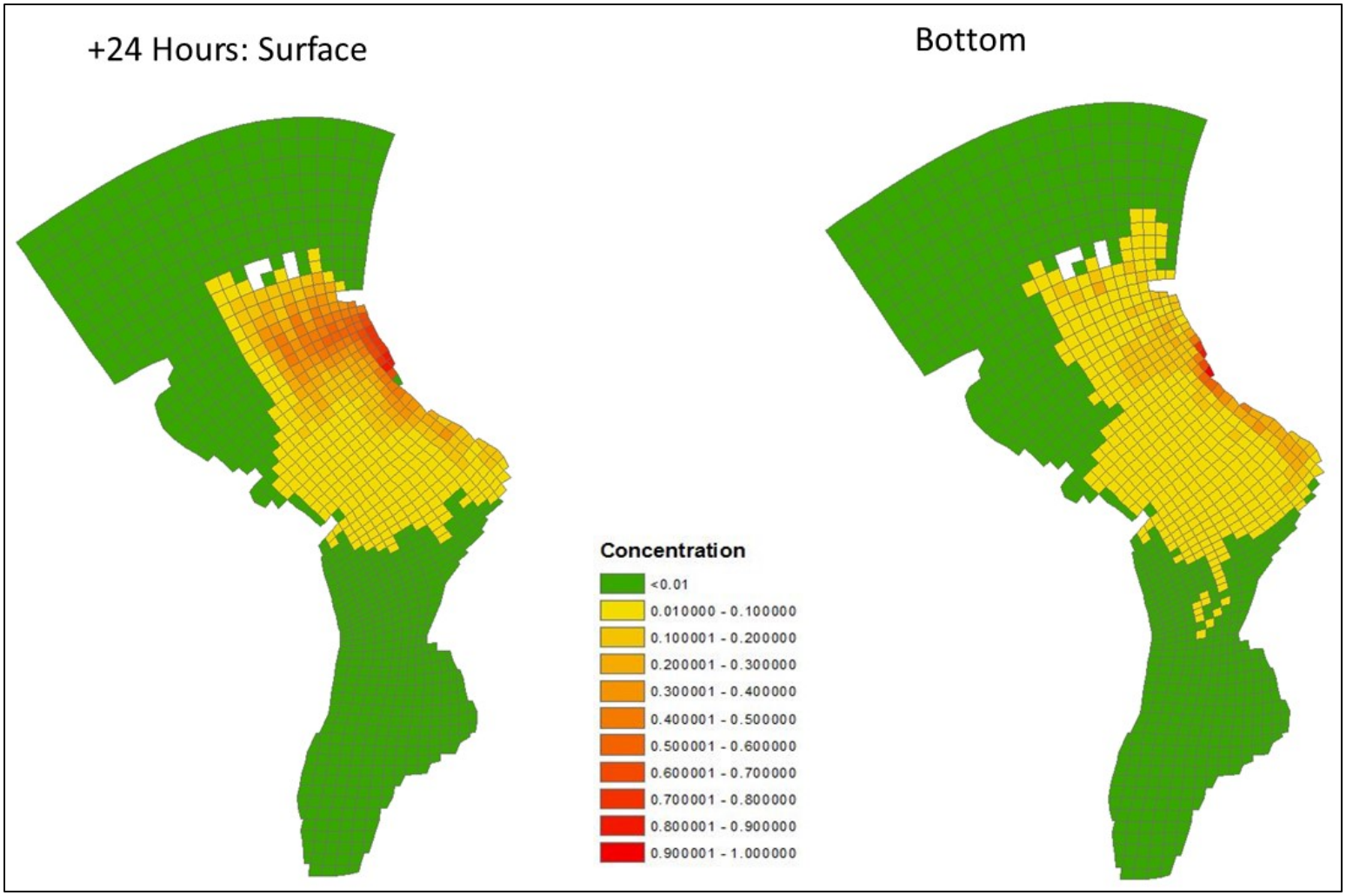

Figure 32. Tracer discharge and vertical mixing study: tracer concentrations in surface and bottom layer at 24 hours.

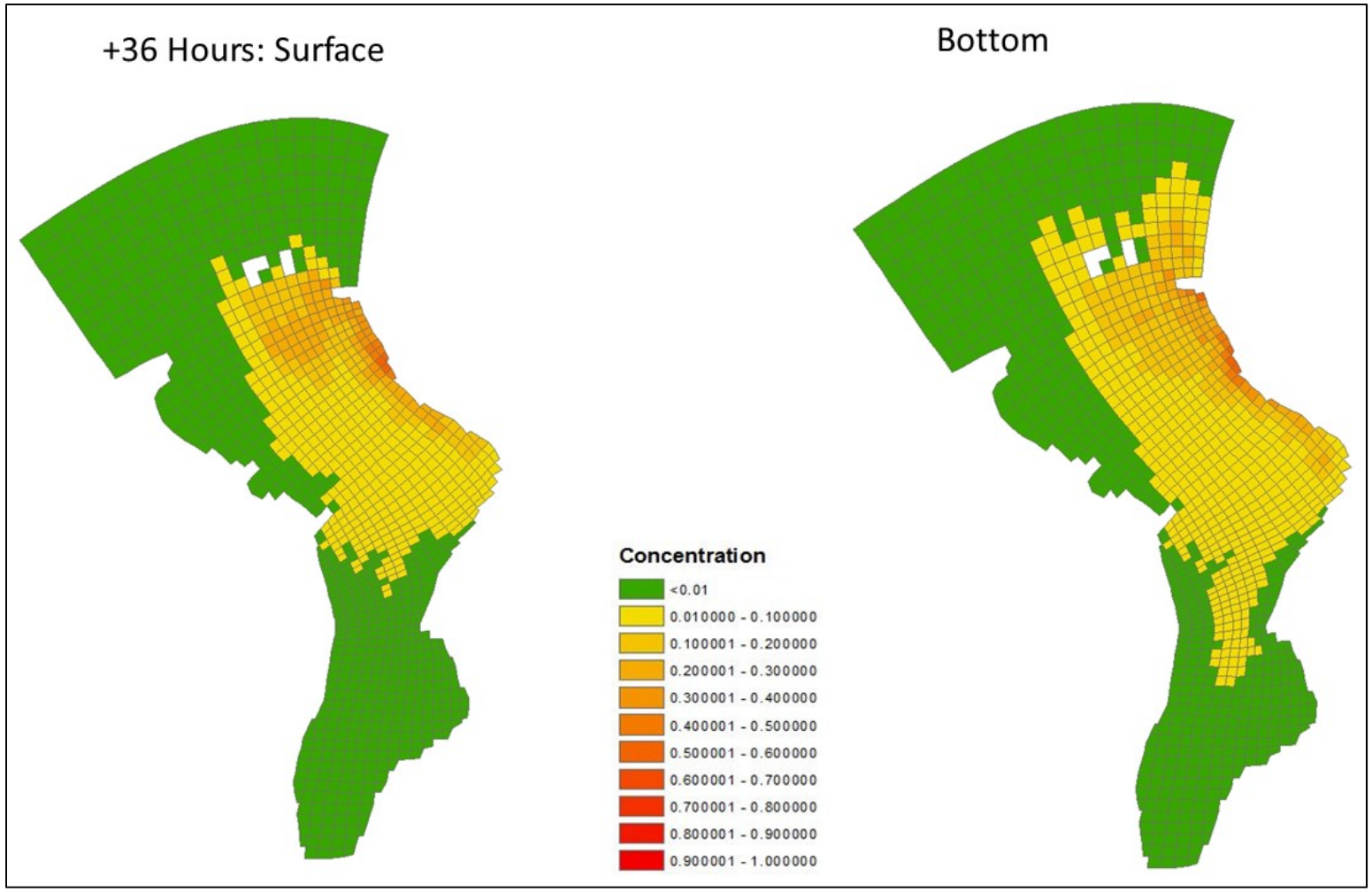

Figure 33. Tracer discharge and vertical mixing study: tracer concentrations in surface and bottom layer at 36 hours.

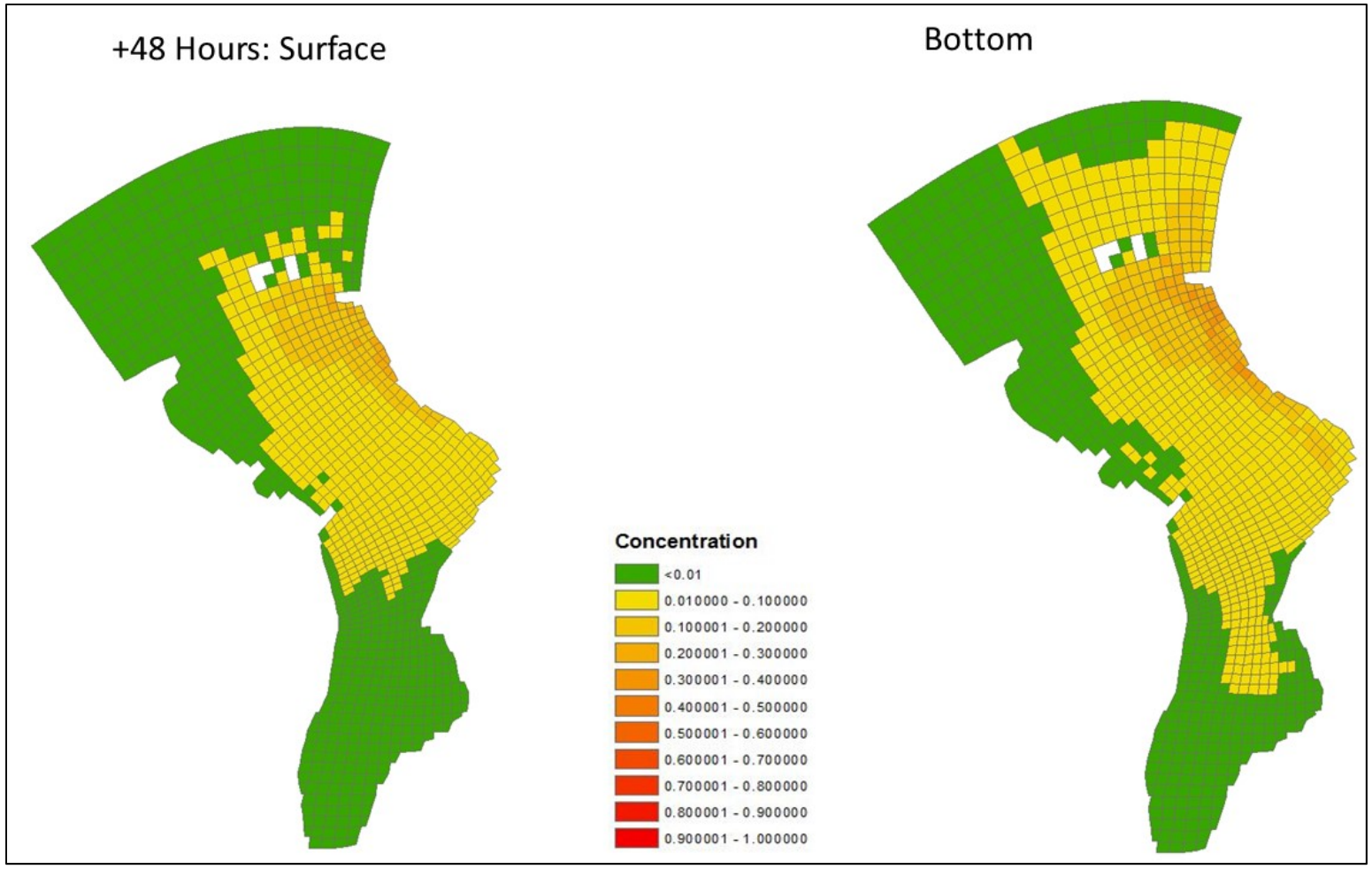

Figure 34. Tracer discharge and vertical mixing study: tracer concentrations in surface and bottom layer at 48 hours.

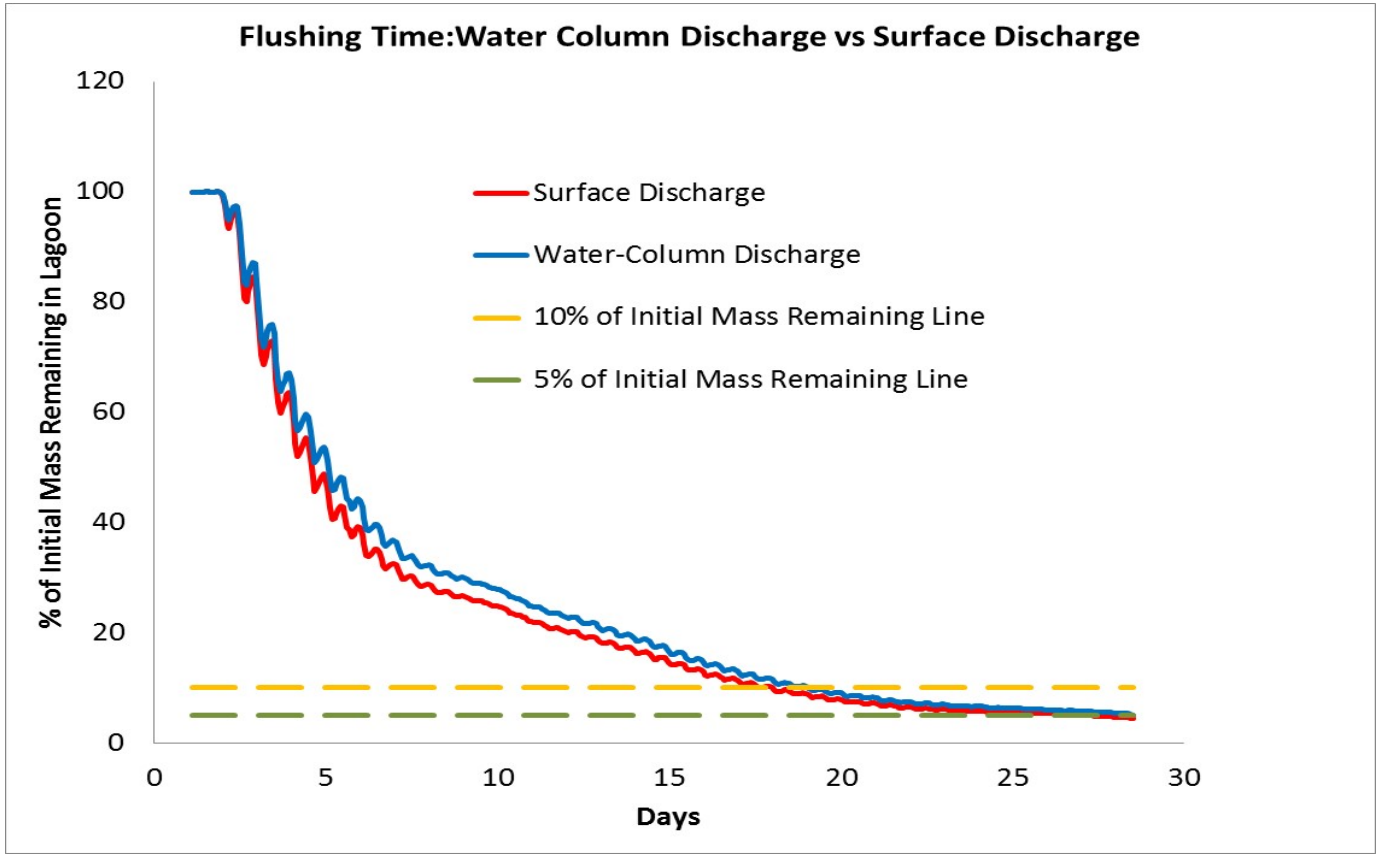

Figure 35. Total mass remaining in the lagoon for continuous discharge and surface discharge scenarios.

5. SUMMARY AND CONCLUSIONS

A modeling and field study was conducted to better understand the hydrodynamic characteristics of the Diego Garcia Lagoon. The study included model–data comparisons for several key variables, including water surface elevation, currents, salinity, and temperature. The predictive capability of the hydrodynamic EFDC model was applied to prediction of flushing time and vertical mixing characteristics of the different regions of the lagoon.

Hydrodynamically, the lagoon can be thought of as three broad regions, the outer lagoon, the mid-lagoon, and the inner lagoon (Figure 36). The outer lagoon is characterized by strong tidal flushing, which is estimated to be 19 to 25 days, weak estuarine circulation, and saltier and cooler water temperature. This results in effective flushing of much of the released mass prior to complete vertical mixing in the water column. The inner lagoon is characterized by shallower water depth, which was sensitive to the freshwater inflows to the region during precipitation. As a result, this region was characterized by warmer, fresher water with moderate estuarine circulations and weak tidal influence. Flushing time in this region was estimated to be 38 to 43 days, the longest of all three regions. The mid-lagoon connects the outer lagoon and the inner lagoon, thus possessing transitional characteristics, including moderate tidal flushing and estuarine circulation.

In the designed discharge scenario in the outer region, vertical mixing in the water column was estimated to complete in about 3 to 4 days. Flushing times were estimated to be 19 to 28.5 days, and 17.6 to 27 days for the water-column discharge and the surface discharge scenario, respectively, with 1.5 days shorter for the surface discharge than for the water-column discharge scenario.

It was estimated that only 3.5% of the total discharge mass ends up to the bottom layer for the continuous discharge scenario for a surface discharge. If discharge were to take place only during slack high tide, which conceptually would tend to flush out of the lagoon by the subsequent ebbing tide, only 2.4% of the total discharge mass ends up to the bottom layer, a reduction of 1% of the total discharge mass from the continuous discharge scenario. Figure 36 summarizes the findings of the study and the influence of lagoon processes on the flushing rate of ship discharges. For releases to the surface water of the outer lagoon, strong tidal flushing tends to disperse and discharge the majority of the mass release prior to completing vertical mixing.

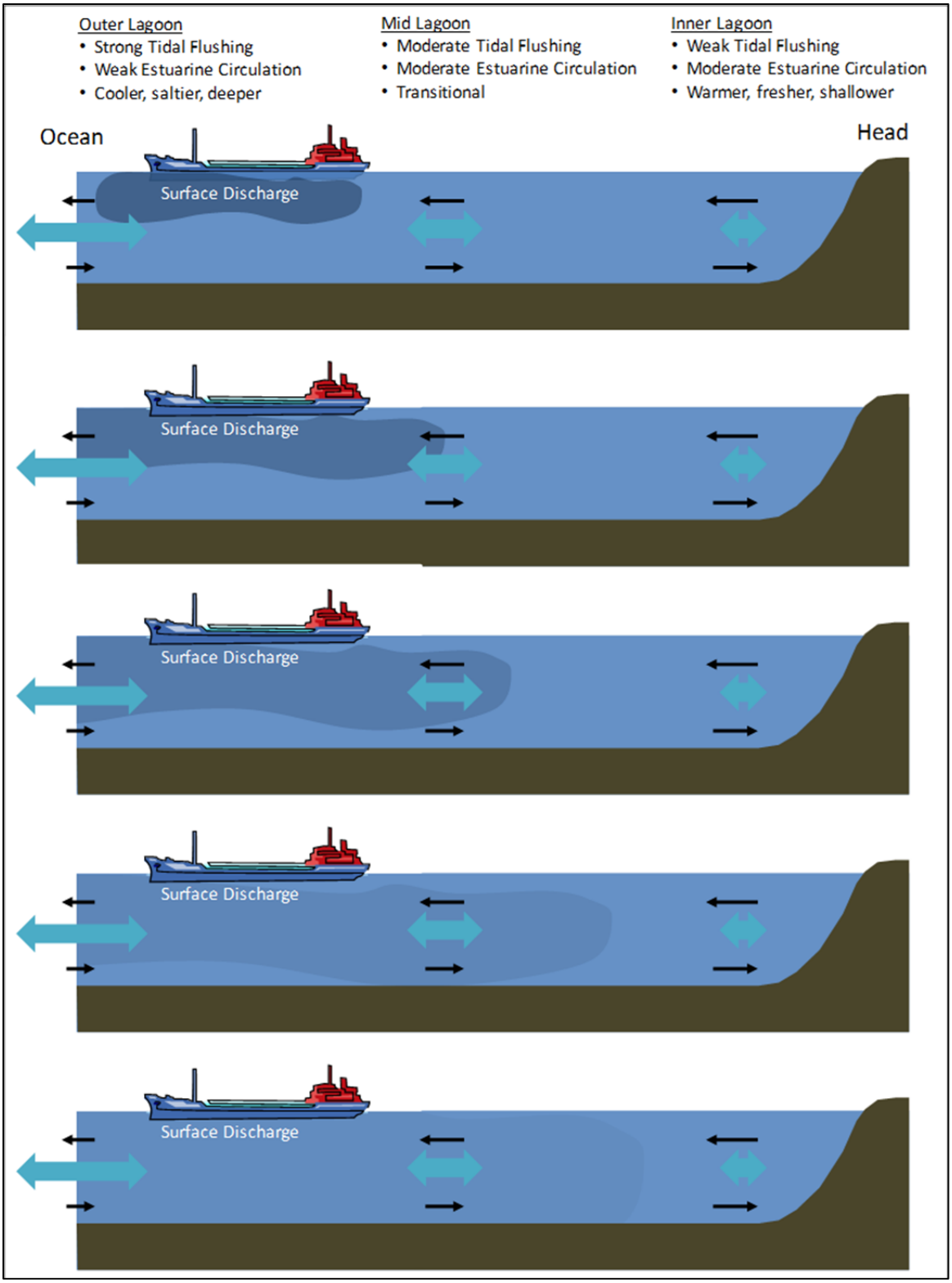

Figure 36. Conceptual model of the processes influencing the flushing rate of surface discharges from ships in the outer region of Diego Garcia Lagoon.

REFERENCES

CIMIS-Penman Equation. 2014. Available at http://www.cimis.water.ca.gov/.

Hansen, D. V. and M. Rattray Jr. 1966. "New Dimensions in Estuary Classification," *Limnology and Oceanography*, vol. XI, no. 3 (July), pp. 319–326.

Lawrence, M. G. 2005. "The Relationship between Relative Humidity and the Dewpoint Temperature in Moist Air: A Simple Conversion and Applications," *Bulletin of the American Meteorological Society* vol. 86, pp. 225–233.

APPENDIX A

CTD DATA TABLES

Table A-1. Station locations of CTD vertical profiles measurements (Set 1 Axial). Positions are based on the average value recorded when the unit was at the surface, at mid-depth, and at the bottom.

Station	Date	Latitude (S)	Longitude (E)	Depth (m)
VP1-1	3/6/2014 11:03	-7.24581906	72.38938367	10.6
VP-ADCP1	3/6/2014 11:18	-7.25279868	72.40508714	21.6
VP1-3	3/6/2014 11:30	-7.25766502	72.40397903	23.2
VP1-4	3/6/2014 11:42	-7.26335319	72.41105348	22.2
VP1-5	3/6/2014 11:55	-7.26887405	72.41853672	21.5
VP1-6	3/6/2014 12:07	-7.27433167	72.42537792	27.0
VP1-7	3/6/2014 12:20	-7.27952504	72.43343794	24.0
VP1-8	3/6/2014 12:31	-7.28516345	72.44033559	27.5
VP1-9	3/6/2014 12:43	-7.29274817	72.44623628	26.5
VP1-10	3/6/2014 12:54	-7.30143013	72.44962691	25.8
VP1-11	3/6/2014 12:54	-7.30909328	72.45310531	27.5
VP1-ADCP2	3/6/2014 13:16	-7.31417856	72.45036156	24.5
VP1-13	3/6/2014 13:28	-7.32785200	72.45372535	13.0
VP1-ADCP3	3/6/2014 13:37	-7.33855634	72.44923132	15.1
VP1-14	3/6/2014 13:45	-7.34530493	72.45353897	11.3
VP1-15	3/6/2014 13:54	-7.35418008	72.45344647	13.8
VP1-16	3/6/2014 14:14	-7.36365071	72.45416893	17.0
VP1-ADCP4	3/6/2014 14:24	-7.37181063	72.45071856	17.0
VP1-18	3/6/2014 14:34	-7.38158158	72.45234572	16.3
VP1-19	3/6/2014 14:44	-7.39000875	72.44882273	10.8
VP1-20	3/6/2014 14:56	-7.39780879	72.44469529	19.5
VP1-ADCP5	3/6/2014 15:07	-7.40403129	72.43691469	12.4
VP1-22	3/6/2014 15:16	-7.41343286	72.43569589	15.5
VP1-23	3/6/2014 15:23	-7.42214742	72.43496583	5.0

Table A-2. Station locations of CTD vertical profiles measurements (Set 1 Cross-Lagoon). Positions are based on average value recorded when the unit was at the surface, at mid-depth, and at the bottom.

Station	Date	Latitude (S)	Longitude (E)	Depth m
VP1-26	3/7/2014 10:43	-7.29316193	72.41870694	20.2
VP1-27	3/7/2014 10:51	-7.29283245	72.42781185	25.8
VP1-28	3/7/2014 10:59	-7.29282828	72.43692238	20.9
VP1-29	3/7/2014 11:06	-7.29278436	72.44623156	26.8
VP1-30	3/7/2014 11:15	-7.292558778	72.4552794	28.4
VP1-31	3/7/2014 11:23	-7.292265544	72.46403159	26.8
VP1-32	3/7/2014 11:32	-7.292600606	72.47272449	25.9
VP1-33	3/7/2014 11:45	-7.2909805	72.4813111	16.9
VP1-34	3/7/2014 13:21	-7.371236017	72.43537695	3.1
VP1-35	3/7/2014 13:28	-7.37175385	72.44405117	16.0
VP1-ADCP4x	3/7/2014 13:38	-7.37194338	72.45019748	17.7
VP1-36	3/7/2014 13:48	-7.372975883	72.46310049	18.2
VP1-37	3/7/2014 13:58	-7.373813992	72.47225228	13.0
VP1-38	3/7/2014 14:22	-7.406585908	72.44882207	2.6
VP1-ADCP5x	3/7/2014 14:30	-7.404160683	72.43659092	15.2
VP1-39	3/7/2014 14:41	-7.404234608	72.43009855	7.7
VP1-40	3/7/2014 15:06	-7.4046152	72.42304747	1.4

Table A-3. Station locations of CTD vertical profiles measurements (Set 2 Axial). Positions are based on average value recorded when unit was at surface, at mid-depth, and at bottom.

Station	Date	Latitude (S)	Longitude (E)	Depth (m)
VP2-Ocean	3/11/2014 8:55	-7.239334083	72.38915658	13.0
VP2-ADCP1	3/11/2014 9:12	-7.25322023	72.40309340	15.9
VP2-ADCP2	3/11/2014 9:34	-7.31510859	72.45276067	21.2
VP2-ADCP3	3/11/2014 9:51	-7.33847575	72.44911453	11.2
VP2-ADCP4	3/11/2014 10:03	-7.37150933	72.45029226	18.7
VP2-ADCP5	3/11/2014 10:19	-7.40354500	72.43666567	7.0

Table A-4. Station locations of CTD vertical profiles measurements (Set 3 Axial). Positions are based on the average value recorded when the unit was at the surface, at mid-depth, and at the bottom.

Station	Date	Latitude (S)	Longitude (E)	Depth (m)
VP3-Ocean	3/13/2014 8:51	-7.238641528	72.38937559	28.0
VP3-ADCP1	3/13/2014 9:04	-7.25298533	72.40287790	18.6
VP3-ADCP2	3/13/2014 9:30	-7.31517205	72.45280577	22.9
VP3-ADCP3	3/13/2014 9:48	-7.33850744	72.44896823	10.9
VP3-ADCP4	3/13/2014 10:01	-7.37149433	72.45060002	18.1
VP3-ADCP5	3/13/2014 11:05	-7.40378438	72.43642822	7.1
VP3-19	3/13/2014 12:25	-7.38849619	72.44941849	20.3

Table A-5. Station locations of CTD vertical profiles measurements (Set 4 Axial). Positions are based on the average value recorded when the unit was at the surface, at mid-depth, and at the bottom.

Station	Date	Latitude (S)	Longitude (E)	Depth (m)
VP4-Ocean	3/18/2014 8:19	-7.239864218	72.39010876	11.7
VP4-ADCP1	3/18/2014 8:32	-7.25265683	72.40291164	19.8
VP4-ADCP2	3/18/2014 9:00	-7.31509945	72.45244632	21.8
VP4-ADCP3	3/18/2014 9:15	-7.33850556	72.44894122	9.2
VP4-ADCP4	3/18/2014 9:30	-7.37186796	72.45010796	17.8
VP4-ADCP5	3/18/2014 9:48	-7.40388974	72.43669249	8.7
Turtle Cove	3/18/2014 10:00	-7.42790077	72.43418533	sfc

REPORT DOCUMENTATION PAGE

Form Approved
OMB No. 0704-01-0188

PLEASE DO NOT RETURN YOUR FORM TO THE ABOVE ADDRESS.

1. REPORT DATE *(DD-MM-YYYY)*	2. REPORT TYPE	3. DATES COVERED *(From - To)*
September 2014	Final	

4. TITLE AND SUBTITLE

Hydrodynamic Modeling of Diego Garcia Lagoon

Final Report

5a. CONTRACT NUMBER

5b. GRANT NUMBER

5c. PROGRAM ELEMENT NUMBER

6. AUTHORS

P.F. Wang
C. N. Katz
D. B. Chadwick
R. Barua

5d. PROJECT NUMBER

5e. TASK NUMBER

5f. WORK UNIT NUMBER

7. PERFORMING ORGANIZATION NAME(S) AND ADDRESS(ES)

SSC Pacific, 53560 Hull Street, San Diego, CA 92152–5001

8. PERFORMING ORGANIZATION REPORT NUMBER

TR 2046

9. SPONSORING/MONITORING AGENCY NAME(S) AND ADDRESS(ES)

Naval Facilities Engineering Command Headquarters
1322 Patterson Avenue, SE, Suite 1000
Washington Navy Yard 20374-5065

10. SPONSOR/MONITOR'S ACRONYM(S)

11. SPONSOR/MONITOR'S REPORT NUMBER(S)

NAVFAC-HQ

12. DISTRIBUTION/AVAILABILITY STATEMENT

Approved for public release.

13. SUPPLEMENTARY NOTES

14. ABSTRACT

A modeling and field study was conducted to better understand the hydrodynamic characteristics of the Diego Garcia Lagoon. The study included model–data comparisons for several key variables, including water surface elevation, currents, salinity, and temperature. The predictive capability of the hydrodynamic Environmental Fluid Dynamics Code (EFDC) model was applied to prediction of flushing time and vertical mixing characteristics of the different regions of the lagoon. It was estimated that only 3.5% of the total discharge mass ends up to the bottom layer for the continuous discharge scenario for a surface discharge. If discharge were to take place only during slack high tide, which conceptually would tend to flush out of the lagoon by the subsequent ebbing tide, only 2.4% of the total discharge mass ends up to the bottom layer, a reduction of 1% of the total discharge mass from the continuous discharge scenario. For releases to the surface water of the outer lagoon, strong tidal flushing tends to disperse and discharge the majority of the mass release prior to completeing vertical mixing.

15. SUBJECT TERMS

Mission Area: Environmental Science

hydrodynamic modeling	flushing time estimates	ataloggers	stratification
Environmental Fluid Dynamics Code	acoustic Doppler current profilers	water surface elevation	vertical mixing

16. SECURITY CLASSIFICATION OF:			17. LIMITATION OF ABSTRACT	18. NUMBER OF PAGES	19a. NAME OF RESPONSIBLE PERSON
a. REPORT	b. ABSTRACT	c. THIS PAGE			C. N. Katz
U	U	U	U	66	19B. TELEPHONE NUMBER *(Include area code)* (619) 553-5332

INITIAL DISTRIBUTION

84300	Library	(2)
85300	Archive/Stock	(1)
71705	D.B. Chadwick	(1)
71750	C. N. Katz	(19)
71750	R. Ripan	(1)
71750	P.F. Wang	(1)

Defense Technical Information Center
Fort Belvoir, VA 22060–6218 (1)

Approved for public release.

SSC Pacific
San Diego, CA 92152-5001